

# FedMT: Federated Learning with Mixed-type Labels

Qiong Zhang\*

Department of Statistics  
The University of British Columbia  
Institute of Statistics and Big Data  
Renmin University of China  
qiong.zhang@ruc.edu.cn

Aline Talhouk

Department of Obstetrics & Gynecology  
The University of British Columbia  
a.talhouk@ubc.ca

Gang Niu

RIKEN  
gang.niu.ml@gmail.com

Xiaoxiao Li†

Department of Electrical and Computer Engineering  
The University of British Columbia  
xiaoxiao.li@ece.ubc.ca

November 21, 2022

## Abstract

In *federated learning* (FL), classifiers (e.g., deep networks) are trained on datasets from multiple centers without exchanging data across them, and thus improves *sample efficiency*. In the classical setting of FL, the *same labeling criterion* is usually employed across all centers being involved in training. This constraint greatly limits the applicability of FL. For example, standards used for *disease diagnosis* are more likely to be different across clinical centers, which mismatches the classical FL setting. In this paper, we consider an important yet under-explored setting of FL, namely FL with *mixed-type labels* where *different labeling criteria* can be employed by various centers, leading to inter-center label space differences and challenging existing FL methods designed for the classical setting. To effectively and efficiently train models with mixed-type labels, we propose a theory-guided and model-agnostic approach that can make use of the underlying correspondence between those label spaces and can be easily combined with various FL methods such as FedAvg. We present *convergence analysis* based on over-parameterized ReLU networks. We show that the proposed method can achieve linear convergence in label projection, and demonstrate the impact of the parameters of our new setting on the convergence rate. The proposed method is evaluated and the theoretical findings are validated on benchmark and medical datasets.

## 1 Introduction

Federated learning (FL) enables centers to jointly learn a model while keeping data at each center. It avoids the centralization of data which is restricted by regulations such as CCPA (Legislature, 2018), HIPAA (Act, 1996), and GDPR (Voigt et al., 2018) and has gained popularity in various applications. The widely used FL methods, such as FedAvg (McMahan et al., 2017), FedAdam (Reddi et al., 2020), and others use iterative optimization algorithms to achieve jointly model training across centers. At each round, local center performs stochastic gradient descent (SGD) for several steps then centers communicate their current model weight to a central server to be aggregated.

When training a classifier in the classical FL setting, the datasets across all centers are annotated with the same labeling criterion. However, in real applications such as healthcare, standards for disease diagnosis may be different across clinical centers due to varying levels of expertise or technology available at different sites. For example, when diagnosing ADHD with brain imaging, the labels are usually acquired over a long period of behavior studies. Different centers may follow different diagnosis and statistical manuals (McKeown et al., 2015) and it is difficult to ask centers to relabel data using a unified criterion as some behavior studies cannot be repeated. This leads to different label spaces across centers. In addition, the center with the most complex labeling criterion, whose label space is desired for future

\*Work done while transitioning to Renmin university of China.

†Corresponding to: Xiaoxiao Li (xiaoxiao.li@ece.ubc.ca).

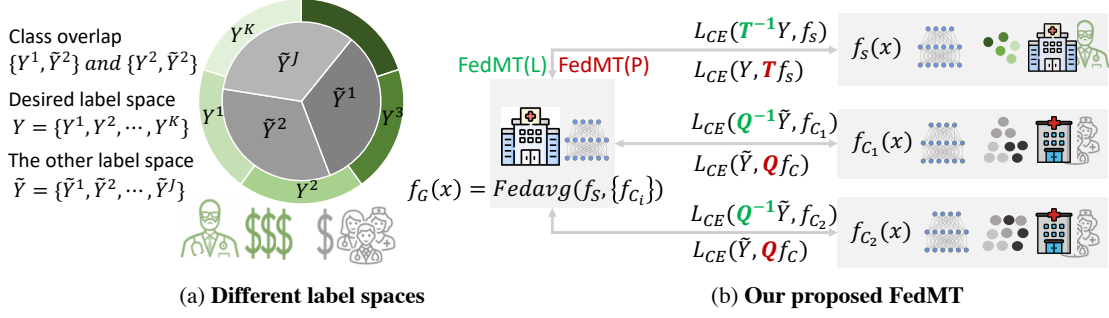


Figure 1: Illustration of the problem setting and our proposed FedMT method. (a) We consider different label spaces (*i.e.*, desired label space  $\mathcal{Y}$  with  $K$  classes and the other space  $\tilde{\mathcal{Y}}$  with  $J$  classes) where classes may overlap, such as  $Y^1$  and  $\tilde{Y}^2$ . Annotation using the desired label criterion is usually harder and more expensive to obtain, thus less such labeled samples are available. (b) We use fixed label space correspondence matrix  $\mathbf{Q}$  to associate label spaces  $\tilde{\mathcal{Y}}$  with  $\mathcal{Y}$  and noise correction matrix  $\mathbf{T}$  to correct label noises in  $\mathcal{Y}$  (if any). We correct predictions by multiplying classifiers’ probability output  $f$  by projection matrices locally (FedMT (P)) or correct labels by multiplying by the inverse of projection matrices to sample observed labels (FedMT (L)) under FedAvg framework.

prediction, typically only has limited labeled samples due to labeling difficulty or cost. In this paper, we aim to answer the following important question:

*With limited samples from the desired label space, how to leverage the commonly used FL pipeline (e.g., FedAvg) and data from other centers in different label spaces to jointly learn an FL model in the desired label space, without additional feature exchanging and data relabeling?*

**Problem Setting:** We study an FL problem for a given classification task. Each center has one labeling criterion, and the criteria across centers can be different. Samples do not overlap across centers. As shown in Fig. 1, first, label spaces are **not** necessarily nested. One class from the desired space may overlaps with different classes in another space and vice versa (*e.g.*, disease diagnoses often exhibit imperfect agreement). Second, following the motivated healthcare example, we assume *limited* amount of labeled data ( $< 5\%$ ) in the *desired label space* is available<sup>1</sup>. Moreover, for the ease of experiment design, we consider the case where these data are stored in one ‘*specialized center*,’ and this center can be treated as the server to coordinate FL but still perform local model updating like the other clients, *i.e.*, the centers with the other labeling criteria. All the centers jointly train an FL model following the standard FL training protocol as shown in Fig. 1 (b).

Prior methods for dealing with different labels spaces include personalized FL (Collins et al., 2021), but they fail to leverage the correspondence across different label spaces. Transfer learning (Yang et al., 2019) which pretrains a model on one space and finetunes the pretrained model on other spaces can be an alternative solution in FL, but sub-optimal pretraining may lead to negative transfer (Chen et al., 2019). Therefore, to address the limitation of above methods, we want to a) simultaneously leverage different types of labels and their correspondence and b) learn FL model end-to-end. To the best of our knowledge, other possible centralized methods meet our needs a) and b) are restricted to coarse to fine label spaces that have hierarchical structures (Touvron et al., 2021; Chen et al., 2021a), which does not hold for the general problem of our interest, or require pulling all data features together for similarity comparison using more sophisticated training strategies (Hu et al., 2022). These methods cannot be simply extended to widely used FL methods (*e.g.*, FedAvg) and require feature sharing across centers which increases privacy risks.

To address the above limitations, we propose a plug-and-play method called FedMT, which is a versatile strategy that can be easily combined with various FL pipelines such as FedAvg. Specifically, we use models with the same architecture whose output dimension is the number of classes in the desired label space across all centers. To use client data from the other label space for supervision, we align two spaces either with label (probability) projection that projects the label (class scores) to the other space. We further show that our methods has the bonus to handle label noise. **Contributions:** Our contributions are three folds. *Methodologically*, we propose a novel FL method, FedMT, which is a computationally efficient and versatile solution *Theoretically*, we present the convergence of FedMT in FL with over-parameterized ReLU neural networks, and explore the impact of amount of data from desired label space and different noise levels; *Empirically*, we demonstrate the superior results in this challenging setting over prior art with extensive experiments on benchmark and medical datasets.

<sup>1</sup>Due to labeling difficulties, such labels can also be noisy. Hence, we also explore this property in our work.

## 2 Related Work

**Federated learning** FL is emerging as a learning paradigm for distributed clients that bypasses data sharing to train local models collaboratively. To aggregate model parameters, FedAvg (McMahan et al., 2017) is the most widely used approach in FL. Variants of FedAvg have been proposed to improve optimization (Reddi et al., 2020; Rothchild et al., 2020) and for non-iid data (Li et al., 2021, 2020a; Karimireddy et al., 2020). Recently FL methods have been studied in semi-supervised learning (Jeong et al., 2021; Bdair et al., 2021), weakly supervised learning (Lu et al., 2021), and positive label only learning (Yu et al., 2020). Theoretical studies of FL have not yet directly addressed neural network algorithms nor accounted for the influence of individual data samples (Karimireddy et al., 2020; Li et al., 2019; Khaled et al., 2020). Recently, a theoretical framework for FL on fully supervised neural network regression using FedAvg was proposed in Huang et al. (2021). To the best of our knowledge, this is the first work to investigate FL’s theory on neural network classification under mixed-type labeled data.

**Neural Tangent Kernel (NTK)** NTK is an essential tool to study the learnability of neural networks. NTK was first studied by Jacot et al. (2018) showing the equivalence between training an infinitely wide neural network with gradient descent and kernel regression. NTK theory has been extended to convolutional neural networks (CNNs) (Arora et al., 2019), graph neural networks (GNNs) (Du et al., 2019; Jiang et al., 2019), recurrent neural networks (RNNs) (Alemohammad et al., 2020). NTK for FL was recently studied by Huang et al. (2021), in the supervised FL regression problem using mean squared error loss.

## 3 Methods

### 3.1 Preliminaries: Classical FL

We start by reviewing the classical FL approach, FedAvg, with full supervision (McMahan et al., 2017) for classification with the same labeling criterion. We consider a  $K$ -class classification problem with the feature space  $\mathcal{X}$  and the label space  $\mathcal{Y} = [K]$ . Let  $\mathbf{x} \in \mathcal{X}$  and  $y \in \mathcal{Y}$  be the input and output random variables following an underlying joint distribution with density  $p(\mathbf{x}, y)$ . Let  $\mathbf{f} : \mathcal{X} \rightarrow \mathbb{R}^K$  be a  $K$ -class classifier such that  $\sigma(\mathbf{f}_k(\mathbf{x})) = p(y = k|\mathbf{x})$ , where  $f_k(\mathbf{x})$  is the  $k$ -th element of  $\mathbf{f}(\mathbf{x})$  and  $\sigma(\mathbf{f}_k) = \exp(f_k) / \sum_{k'=1}^K \exp(f_{k'})$  is the softmax function. Then the predicted label can be obtained via  $y_{\text{pred}} = \arg \max_{k \in [K]} f_k(\mathbf{x})$ .

In the classical FL setup, each client  $c \in [C]$  has access to a labeled training set  $\mathcal{D}_c = \{(\mathbf{x}_i^c, y_i^c)\}_{i=1}^{N_c}$  of size  $N_c$  and learns its local model  $\mathbf{f}^c$  by minimizing the following empirical risk:

$$\hat{R}_c^a(\mathbf{f}^c; \mathcal{D}_c) = \frac{1}{N_c} \sum_{i=1}^{N_c} \ell(\mathbf{f}^c(\mathbf{x}_i^c), y_i^c), \quad (1)$$

where  $\ell$  is the *cross-entropy loss*, i.e.,  $\ell_{\text{CE}}(\mathbf{f}^c(\mathbf{x}), y) = -\sum_{k=1}^K \mathbb{1}(y = k) \log f_k^c(\mathbf{x}) = -\log f_y^c(\mathbf{x})$  and  $\mathbb{1}(\cdot)$  is the indicator function.

The goal of classical FL is that  $C$  clients collaboratively train a global classification model  $\mathbf{f}$  that generalizes well with respect to  $p(\mathbf{x}, y)$ , without sharing their local data  $\mathcal{D}_c$ . The problem can be formalized as minimizing the aggregated risk:  $R(\mathbf{f}) = \frac{1}{C} \sum_{c=1}^C \hat{R}_c^a(\mathbf{f}; \mathcal{D}_c)$ . FedAvg employs a server to coordinate the iterative distributed training through model parameter averaging as described in Algorithm 1.

### 3.2 Problem Formulation

In contrast to the classical supervised FL classification, where all the centers share the same label space, we consider the case where the label spaces across centers may be different. For the ease of presentation, we assume there are two label spaces, namely  $\mathcal{Y} = \{Y^k\}_{k=1}^K$  and  $\tilde{\mathcal{Y}} = \{\tilde{Y}^j\}_{j=1}^J$  where  $K > J$ .<sup>2</sup> For the ‘specialized center’ with the desired label space, we denote it as a server and its dataset as  $\mathcal{D}^s = \{(\mathbf{x}_i^s, y_i^s) : i \in [nK]\}$ , where  $y_i^s \in \mathcal{Y}$ . We also have in total  $N$  labeled data with a different criterion that are stored across  $C$  clients. For  $c \in [C]$ , we denote by  $S_c$  the indices of data from the other label space  $\mathcal{D}^c = \{(\mathbf{x}_i^c, y_i^c) : i \in S_c\}$  on  $c$ -th client, where  $y_i^c \in \tilde{\mathcal{Y}}$ . Let  $N_c = |S_c|$  and we have  $N = \sum_{c \in [C]} N_c$ . Our objective is to train a global classifier in the desired label space  $\mathbf{f} : \mathcal{X} \mapsto \mathcal{Y}$  using data in the system from different label spaces.

<sup>2</sup>Our method can be easily extended to multiple label spaces.

### 3.3 Proposed Method

**Motivation** Learning under different label spaces can be formulated as a corrupted label learning problem (Van Rooyen and Williamson, 2017; Patrini et al., 2017), where label space with less classes  $\tilde{\mathcal{Y}}$  is treated as the corrupted observation of a true underlying label space  $\mathcal{Y}$  with more classes, *i.e.*, our desired label space. Our method is based on loss correction (Van Rooyen and Williamson, 2017; Patrini et al., 2017), which is a well-established corrupted label learning approach in the centralized domain with statistically consistency guarantees.

Let  $\mathbb{T} : \mathcal{Y} \mapsto \tilde{\mathcal{Y}}$  be a linear transformation, whose pseudo inverse is  $\mathbb{T}^{-1}$ . Under proper assumptions (see Theorem 3.1) and a given function  $\mathbf{f} : \mathcal{X} \mapsto \mathcal{Y}$ , Patrini et al. (2017) showed two ways to perform loss correction that  $\mathbb{T}^{-1}$  can pull back from functions of corrupted labels to functions of true labels and  $\mathbb{T}$  can transfer functions of true labels to those of corrupted labels. Mathematically, this can be written as:

**Theorem 3.1** (Loss correction (informal) (Patrini et al., 2017; Van Rooyen and Williamson, 2017)). *Given a non-singular linear mapping matrix  $\mathbb{T}$  and a proper loss  $\ell$ , one can achieve the same minimizer of the original loss under the true label distribution:*

$$\arg \min_{\mathbf{f}} \mathbb{E}_{\mathbf{x}, \mathbf{y} \in \mathcal{Y}} \ell(\mathbf{y}, \mathbf{f}) = \arg \min_{\mathbf{f}} \mathbb{E}_{\mathbf{x}, \mathbf{y} \in \tilde{\mathcal{Y}}} \ell(\mathbf{y}, \mathbb{T}\mathbf{f}) \quad \text{and} \quad \mathbb{E}_{\mathbf{x}, \mathbf{y} \in \mathcal{Y}} \ell(\mathbf{y}, \mathbf{f}) = \mathbb{E}_{\mathbf{x}, \mathbf{y} \in \tilde{\mathcal{Y}}} \mathbb{T}^{-1} \ell(\mathbf{y}, \mathbf{f}).$$

In addition, loss correction methods are model agnostic and can be generalized to many loss functions, therefore provide a versatile framework for learning from corrupted labels. Since our goal is to jointly learn a classifier  $\mathbf{f} : \mathcal{X} \rightarrow \mathbb{R}^K$  for clients and server, the overall loss can be written as:

$$R_{\text{overall}}(\mathbf{f}) = \frac{1}{C+1} \left\{ \hat{R}_s(\mathbf{f}) + \sum_{c=1}^C \hat{R}_c(\mathbf{f}; \mathcal{D}^c) \right\}, \quad (2)$$

where  $\hat{R}_s(\mathbf{f})$  and  $\hat{R}_c(\mathbf{f})$  are respectively the empirical risk based on the server's data and the clients' data from a different label space. To minimize the overall loss in (2), we need to align the predictions or losses of both types of labels to the underlying true label space. Considering the specific form of cross-entropy (1), we adapt the findings of Patrini et al. (2017); Van Rooyen and Williamson (2017) to our FL setting. For all the clients in FL  $l \in [C]$ , we propose leveraging the following two kinds of projections to both server and clients as:

$$\textbf{Probability projection: } \hat{R}_l(\mathbf{f}; \mathcal{D}^l) = -\frac{1}{N_l} \sum_{i \in S_l} \sum_{j=1}^J \mathbb{1}(y_i = \tilde{Y}^j) \log \left\{ \sum_{k=1}^K \mathbb{T}_{jk}^l \sigma(f_k(\mathbf{x}_i)) \right\}, \quad (3)$$

$$\textbf{Label projection: } \hat{R}_l(\mathbf{f}; \mathcal{D}^l) = -\frac{1}{N_l} \sum_{i \in S_l} \sum_{k=1}^K \left\{ \sum_{j=1}^J \mathbb{T}_{kj}^{-1} \mathbb{1}(y_i = \tilde{Y}^j) \right\} \log \sigma(f_k(\mathbf{x}_i)). \quad (4)$$

For clients, we denote  $\mathbb{T} = \mathbf{Q} \in [0, 1]^{J \times K}$ , whose  $j$ -th row denotes the mixing weights of classes in the desired label space for  $j$ -th class in the other label space. As both probability projection and label projection are performed locally, the overall loss (2) can be optimized using general FL strategies, such as FedAvg (McMahan et al., 2017) used in this work, or other variants like Li et al. (2020a, 2021); Karimireddy et al. (2020). Note our method can be easily extended to more than one centers in the desired label space as shown in Appendix D.5.

**Extension to Noisy Labels** Another advantage of our method is that it has the flexibility to extend to the case where there are noisy observations, that is the label is mislabeled to a wrong one in the same label space. Let us explain with the case where the server has noisy labels. Specifically, on the server, we let  $\mathbb{T} = \mathbf{T} \in [0, 1]^{K \times K}$  be a matrix whose  $(i, j)$ -th element denotes  $p(\tilde{y}^s = Y^j | y^s = Y^i)$  where  $\tilde{y}^s$  is the observed noisy label and  $y^s$  is the true label.

The detailed FedMT algorithm is described in Algorithm 2,  $\mathbf{T} \neq \mathbf{I}^{K \times K}$  under noisy label case and  $\mathbf{T} = \mathbf{I}^{K \times K}$  for noise-free setting. In this algorithm, it is worth noting that FedMT is easy to implement as it only slightly modifies FedAvg as highlighted in blue.

**Algorithm 1** FL using FedAvg (McMahan et al., 2017)

**Server Input:** initial  $\mathbf{f}$ , aggregation step-size  $\mathcal{D}_s = \{\mathbf{x}^s, \mathbf{y}^s\}$  where  $\mathbf{y}^s \in \mathcal{Y}$ , projection matrix  $T$

$\eta_{\text{agg}}$ , and global communication round  $R$

**Client Input:** local model  $\mathbf{f}^c$ , local dataset  $\mathcal{D}_c$ , projection matrices  $\mathbf{Q}$   
SGD step-size  $\eta_{\text{sgd}}$ , and local updating iterations  $t$  (for  $c \in [C]$ )

- 1: For  $r = 1 \rightarrow R$  rounds, we run **A** on each client and **B** iteratively .
- 2: **procedure A. MODELUPDATE( $r$ )**
- 3:  $\mathbf{f}^c \leftarrow \mathbf{f}$   $\triangleright$  Receive updated model from PROC. B
- 4: **for**  $\tau = 1 \rightarrow t$  **do**
- 5:  $\mathbf{f}^c \leftarrow \mathbf{f}^c - \eta_{\text{sgd}} \cdot \nabla \hat{R}_c^a(\mathbf{f}^c; \mathcal{D}_c)$   $\triangleright$  Model updates via SGD
- 6: send  $\mathbf{f}^c - \mathbf{f}$  to PROC. B
- 7: **procedure B. MODELAGG( $r$ )**
- 8: receive model updates  $\mathbf{f}^c - \mathbf{f}$  from PROC. A
- 9:  $\mathbf{f} \leftarrow \mathbf{f} - \eta_{\text{agg}} \cdot \sum_{c=1}^C (\mathbf{f}^c - \mathbf{f})$
- 10: broadcast  $\mathbf{f}$  to PROC. A

**Algorithm 2** FL using FedMT (Ours)

**Server Input:** inputs of Alg 1, server model  $\mathbf{f}^s$ , *small* noisy dataset

**Client Input:** inputs of Alg 1 but  $\mathcal{D}_c = \{\mathbf{x}^c, \mathbf{y}^c\}$  where  $\mathbf{y}^c \in \tilde{\mathcal{Y}}$ , and projection matrices  $\mathbf{Q}$

- 1: For  $r = 1 \rightarrow R$  rounds, we run **A** on each client and **B** iteratively .
- 2: **procedure A. MODELUPDATE( $r$ )**
- 3:  $\mathbf{f}^c \leftarrow \mathbf{f}$   $\triangleright$  Receive updated model from PROC. B
- 4: **for**  $\tau = 1 \rightarrow t$  **do**
- 5: **if probability projection then**
- 6:  $\mathbf{f}^c \leftarrow \mathbf{f}^c - \eta_{\text{sgd}} \cdot \nabla \hat{R}_c(\mathbf{Q}\mathbf{f}^c; \mathbf{y}^c)$
- 7:  $\mathbf{f}^s \leftarrow \mathbf{f}^s - \eta_{\text{sgd}} \cdot \nabla \hat{R}_s(\mathbf{T}\mathbf{f}^s; \mathbf{y}^s)$
- 8: **else if label projection then**
- 9:  $\mathbf{f}^c \leftarrow \mathbf{f}^c - \eta_{\text{sgd}} \cdot \nabla \hat{R}_c(\mathbf{f}^c; \mathbf{Q}^{-1}\mathbf{y}^c)$
- 10:  $\mathbf{f}^s \leftarrow \mathbf{f}^s - \eta_{\text{sgd}} \cdot \nabla \hat{R}_s(\mathbf{f}^s; \mathbf{T}^{-1}\mathbf{y}^s)$
- 11: send  $\mathbf{f}^l - \mathbf{f}$  to PROC. B for  $l \in \{[C], s\}$
- 12: **procedure B. MODELAGG( $r$ )**
- 13: receive model updates from PROC. A
- 14:  $\mathbf{f} \leftarrow \mathbf{f} - \eta_{\text{agg}} \cdot \sum_{l \in \{[C], s\}} (\mathbf{f}^l - \mathbf{f})$
- 15: broadcast  $\mathbf{f}$  to PROC. A

### 3.4 Theoretical Analysis

Although label projection-based loss correction methods have shown to have good properties under centralized setting (see Theorem 3.1 Patrini et al. (2017); Van Rooyen and Williamson (2017)), their theoretical convergence under FL have not been explored. Hence, we focus on the theoretical analysis of label projection in (4), given it has been shown to have better theoretical guarantees than (3) in a previous study (see Theorem 3.1 (Patrini et al., 2017)). Further, we are interested in investigating the impact of various parameters on theoretical convergence. In this section, we establish a novel theoretical analysis of FedMT using NTK (Arora et al., 2019; Lee et al., 2019; Huang et al., 2021).

**NTK setup** Our theoretical results are studied under an over-parameterized one-hidden layer neural network (NN). Let  $\mathbf{f} : \mathcal{X} \rightarrow \mathbb{R}^K$  be the output of the NN whose  $k$ th element is

$$f_k(\mathbf{u}, \mathbf{x}) = \frac{1}{\sqrt{M}} \sum_{m=1}^M a_{km} \phi(\mathbf{u}_m^\top \mathbf{x})$$

where  $\phi(z) = \max\{z, 0\}$  is the ReLU activation function and  $\mathbf{u} = [\mathbf{u}_1, \mathbf{u}_2, \dots, \mathbf{u}_M] \in \mathbb{R}^{d \times M}$ .

**Definition 3.2** (Initialization). We initialize  $\mathbf{u} \in \mathbb{R}^{d \times M}$  and  $a_{km}$  as follows. For each  $m \in [M]$ ,  $\mathbf{u}_m$  is sampled from  $\mathcal{N}(0, I)$ . For each  $k \in [K]$  and  $m \in [M]$ ,  $a_{km}$  is sampled from  $\{-1, +1\}$  uniformly at random and is not trainable.

In the  $r$ -th global round, the server broadcasts the global model weight  $\mathbf{u}_m(r)$  to every client. Each client  $c$  then starts from  $\mathbf{u}_{m,c}(0, r) = \mathbf{u}(r)$  and takes  $t$  local gradient steps via gradient descent with step size  $\eta_{\text{local}}$

$$\mathbf{u}_{m,c}(\tau + 1, r) = \mathbf{u}_{m,c}(\tau, r) - \eta_{\text{local}} \frac{\partial \hat{R}_c(\mathbf{u}_{m,c}(\tau, r))}{\partial \mathbf{u}_m}$$

where  $\mathbf{u}_{m,c}(\tau, r)$  is the value of  $\mathbf{u}_m$  on  $c$ th client at step  $\tau$  in  $r$ -th global round. Then the client sends  $\Delta \mathbf{u}_{m,c}(r) = \mathbf{u}_{m,c}(t, r) - \mathbf{u}_{m,c}(0, r)$  to server and server computes a new  $\mathbf{u}_{m,c}(r + 1)$  based on the average of all  $\Delta \mathbf{u}_{m,c}(r)$  via

$$\mathbf{u}_m(r + 1) = \mathbf{u}_m(r) + \eta_{\text{agg}} \cdot \sum_{c \in [C]} \Delta \mathbf{u}_{m,c}(r) / C.$$

**NTK analysis results** Let  $g(\mathbf{u}, \mathbf{x}) = \sigma(\mathbf{f}(\mathbf{u}, \mathbf{x}))$  and  $\mathbf{y}_i^c$  be the multi-hot vector representation of  $y_i^c$  and  $\mathbf{y}_i^s$  be the one-hot vector representation of  $y_i^s$  in  $\mathbb{R}^K$ . Let  $\mathbf{Q}$  be the linear mapping from  $\mathcal{Y}$  to  $\tilde{\mathcal{Y}}$  and  $\mathbf{T}$  be the same as before. Following Neural Tangent Kernel (NTK) analysis (Lee et al., 2019; Arora et al., 2019), we consider the mean squared error loss<sup>3</sup> respectively on the client and server

$$\begin{aligned}\hat{R}_c(\mathbf{u}) &= \frac{1}{N_c} \sum_{i \in S_c} \sum_{j=1}^J \sum_{k=1}^K Q_{jk}^{-1} (y_{ik}^c - g_k(\mathbf{u}, \mathbf{x}_i^c))^2, \\ \hat{R}_s(\mathbf{u}) &= \frac{1}{nK} \sum_{i=1}^{nK} \sum_{k'=1}^K \sum_{k=1}^K T_{k'k}^{-1} (y_{ik}^s - g_k(\mathbf{u}, \mathbf{x}_i^s))^2.\end{aligned}\tag{5}$$

**Lemma 3.3.** *Let the notation be the same as before, the NTK kernel  $\mathbf{G}(r)$  based on our proposed novel loss (5) is a block matrix with  $K$  row partitions and  $K$  column partitions. The block matrix in the  $l$ -th row and  $m$ -th column has the following form*

$$\mathbf{G}^{l,m}(r) = \begin{pmatrix} \mathcal{G}_{1,1}^{l,m}(r) & \mathcal{G}_{1,2}^{l,m}(r) & \dots & \mathcal{G}_{1,C}^{l,m}(r) & \mathcal{G}_{1,s}^{l,m}(r) \\ \mathcal{G}_{2,1}^{l,m}(r) & \mathcal{G}_{2,2}^{l,m}(r) & \dots & \mathcal{G}_{2,C}^{l,m}(r) & \mathcal{G}_{2,s}^{l,m}(r) \\ \vdots & \vdots & \ddots & \vdots & \vdots \\ \mathcal{G}_{C,1}^{l,m}(r) & \mathcal{G}_{C,2}^{l,m}(r) & \dots & \mathcal{G}_{C,C}^{l,m}(r) & \mathcal{G}_{C,s}^{l,m}(r) \\ \mathcal{G}_{s,1}^{l,m}(r) & \mathcal{G}_{s,2}^{l,m}(r) & \dots & \mathcal{G}_{s,C}^{l,m}(r) & \mathcal{G}_{s,s}^{l,m}(r) \end{pmatrix}\tag{6}$$

for  $l \in [K]$  and  $m \in [K]$  where each sub-block matrix has the following form:

$$\begin{aligned}\mathcal{G}_{c,j}^{l,m}(t) &= \left\{ \sum_j Q_{jm}^{-1} \right\} \nabla_{\mathbf{u}} g_l(\mathbf{u}(t), \mathcal{D}^c) \nabla_{\mathbf{u}}^\top g_m(\mathbf{u}(t), \mathcal{D}^j), \quad \forall j \in \{[C], s\}, c \in [C] \\ \mathcal{G}_{s,s}^{l,m}(t) &= \left\{ \sum_k T_{km}^{-1} \right\} \nabla_{\mathbf{u}} g_l(\mathbf{u}(t), \mathcal{D}^s) \nabla_{\mathbf{u}}^\top g_m(\mathbf{u}(t), \mathcal{D}^s).\end{aligned}\tag{7}$$

We show detailed derivation of Lemma 3.3. Note that as  $J < K$ ,  $\mathbf{Q} \in \mathbb{R}^{J \times K}$  is not inevitable. In practice, we compute its pseudo inverse instead. Although looking at  $\mathbf{Q}$  alone, the plausible property of Theorem 3.1 may not hold. We claim that by optimizing  $\hat{R}_c(\mathbf{f})$  together with  $\hat{R}_s(\mathbf{f})$ , we benefit from the gradient of labels in the desired label space, as shown in the expression of  $\mathcal{G}_{c,s}^{i,j}(r)$  in Eq. (7).

Following Huang et al. (2021), we further conclude the convergence of the our proposed loss in (5).

**Theorem 3.4** (Convergence). *Let  $M = \Omega(\lambda^{-4}(N + nK)^4 \log((N + nK)/\delta))$ , we iid initialize  $\mathbf{u}_m(0)$ ,  $a_{km}$  as Definition 3.2. Let  $\lambda = \lambda_{\min}(\mathbf{G}(0))$  denote the smallest eigenvalue of  $\mathbf{G}(0)$ . Let  $\kappa$  denote the condition number of  $\mathbf{G}(0)$ . For  $C$  clients, for any  $\epsilon$ , let*

$$R = O\left(\frac{C}{\lambda \eta_{\text{local}} \eta_{\text{agg}} t} \cdot \log(1/\epsilon)\right),$$

$\eta_{\text{local}} = O(\lambda/\kappa t(N + nK)^2)$ , and  $\eta_{\text{agg}} = O(1)$ , the above algorithm satisfies

$$\mathcal{L}(\mathbf{u}(r)) \leq \left(1 - \frac{\eta_{\text{agg}} \eta_{\text{local}} \lambda t}{2C}\right)^r \mathcal{L}(\mathbf{u}(0)).$$

with probability at least  $1 - \delta$ .

The details of the proof are deferred to Appendix B. Note that a smaller value of  $\eta_{\text{agg}} \eta_{\text{local}} \lambda t / 2C$ , e.g., a smaller eigenvalue  $\lambda$  and a larger number of clients, leads to slower convergence. It is clear that  $\lambda$  depends on both  $\mathbf{Q}$  and  $\mathbf{T}$ , therefore it is important to see its connection with  $\mathbf{Q}$  and  $\mathbf{T}$ , we discuss the algorithm convergence under the following two special cases.

**Corollary 3.5** (Convergence under various label granularity differences). *Let  $k_1, k_2, \dots, k_J$  be  $J$  positive integers so that  $K = \sum_{j=1}^J k_j$ . If the transformation from the desired label space to the other label space is  $\mathbf{Q} = \text{diag}(\mathbf{1}_{k_1}^\top, \mathbf{1}_{k_2}^\top, \dots, \mathbf{1}_{k_J}^\top) \in [0, 1]^{J \times K}$  (i.e., the classes in the desired label space are subclasses of classes in the other label space), then the smaller the value of  $J$ , the lower the convergence rate.*

<sup>3</sup>which can be easily extended to the label projection loss

*Proof Sketch:* Based on the form of  $\mathbf{G}(r)$  in (7), it can be seen that (Li et al., 2021)

$$\lambda = \lambda_{\min}(\mathbf{G}(0)) \leq \min_{k,c,s} \{\lambda_{\min}(\mathcal{G}_{c,c}^{k,k}(0)), \lambda_{\min}(\mathcal{G}_{s,s}^{k,k}(0))\} \leq \lambda_{\min}(\mathcal{G}_{c,c}^{k,k}(0)) \lesssim \left\{ \min_j k_j^{-1} \right\} \lambda_0$$

where  $\lambda_0 = \lambda_{\min}(\nabla_{\mathbf{u}} \mathbf{g}(\mathbf{u}(0), \mathcal{D}) \nabla_{\mathbf{u}}^\top \mathbf{g}(\mathbf{u}(0), \mathcal{D}))$ . Since  $\sum_j k_j = K$ , the smaller the value of  $J$ , the smaller the value of  $\lambda$  and hence the algorithm converges slower. See detailed proof in Appendix B.

**Corollary 3.6** (Convergence under different noise levels). *We assume noisy labels are corrupted via*

$$\mathbf{T} = (1 - K/(K-1)\xi) \mathbb{I}_K + \xi/(K-1) \mathbb{I}_K \mathbb{I}_K^\top,$$

where  $T_{ij} = p(\tilde{y}^s = Y_{\mathcal{F}}^j | y^s = Y_{\mathcal{F}}^i)$  with observed noisy label  $\tilde{y}^s$  and true  $y^s$  is the true label, and  $\xi = 1 - T_{ii} \in (0, 1)$  for  $i \in [K]$  denotes the noisy level. In this specified case, the convergence of FedMT with label projection on NTK is does not depend on the noise level  $\xi$ .

*Proof Sketch:* By using matrix inversion lemma, we find  $\mathbf{T}^{-1} = (K-1)/(K-1-K\xi) \mathbb{I}_K - \xi/(K-1-K\xi) \mathbb{I}_K \mathbb{I}_K^\top$ . Hence  $\sum_{k=1}^K T_{kk'} = 1$  for any  $k' \in [K]$ . See Appendix B for details.

## 4 Experiments

In this section, we demonstrate the effectiveness of our proposed method, FedMT, when data are from different label spaces. Compared with other training strategies and prior art, FedMT consistently achieves better test accuracy in predicting labels in the desired label space with limited amount of data from this space as demonstrated on CIFAR100 (Krizhevsky et al., 2009) and a medical dataset.

### 4.1 Benchmark Experiments Setup

**Dataset and setting** We use the CIFAR100 (Krizhevsky et al., 2009) dataset to mimic our proposed problem setting. We assume one center (as server to coordinate FL training) has a small amount of data ( $\leq 5\%$  of total sample size) with sub-class annotations and other centers are labeled using super-class annotations. The sub-class space is viewed as our desired label space. Our objective is to train a classification model using FL to predict sub-class labels with all the centers simultaneously.

The CIFAR100 dataset consists of 50K images, associated with  $K = 100$  sub-classes that could be further grouped into  $J = 20$  super-classes. To study the effect of the number of training samples in desired label space, we randomly select  $n$  observations from each of the 100 sub-classes on the server and the rest of the observations in the training set are split into  $C = 10$  subsets completely at random, ensuring that each class is equally represented in each subset. Each subset corresponds to a dataset stored on one client and we use  $N_c = 4000$ . We use the super-class as our label for all clients. Experiment results with other values of  $C$  and  $N_c$  is given in Appendix D.

We use ResNet18 (He et al., 2016) as our classifier. We use SGD optimizer Ruder (2016) with a learning rate of  $10^{-2}$ , momentum 0.9, and weight decay  $5 \times 10^{-4}$ . The learning rate is divided by 5 at 20, 30, and 40 epochs. If not specified, our default setting for local update epochs is  $E = 1$ . Based on the superclass information in CIFAR100, we are able to formulate the transition matrix  $\mathbf{Q}$  for all clients. Its form and more training details are available in Appendix C.1.

**Baselines** We compare the following approaches: 1) **Single**: only the data from the desired label space is used to train the classifier; 2) **FedMatch** (Jeong et al., 2021): we treat client samples as unlabeled data, perform pseudo-labeling on the unlabeled sets, and augment samples in supervised loss training. 3) **FedRep** (Collins et al., 2021): clients train a  $J$ -class classifier and the server trains a  $K$ -class classifier that differs in the last layer with different output dimension. These classifiers share the same backbone parameters using FedAvg, the performance is tested using the classifier on the server; 4) **FedTrans** (Chen et al., 2021b): all clients trains a  $J$ -class classifier using FedAvg which is later fine-tuned on server with a new  $K$ -class linear layer. We refer **FedMT (P)** as our proposed method with probability projection loss; and refer **FedMT (L)** as our proposed method with label projection loss.

### 4.2 Benchmark Experiments Results

**Comparison under different amount of data on server** We fix number of clients  $C$  at 10, and set different number of samples per-class  $n$  on the server in the range of  $\{5, 10, 15, 20, 25\}$ . The advantage of FL is to enable access to more data to improve model performance. As shown in Tab. 1, when  $n$  increases (supervision information increases), the accuracy of all approaches improves. Both FedMT (P & L) significantly outperform alternative methods when

Table 1: Comparison of the accuracy for 100-class classification using our methods and alternative methods on the CIFAR100 benchmark dataset with different per sub-class number  $n$  images on the server. We report mean (sd) from three trial runs. The best method is highlighted in boldface.

$n$	Single	FedMatch	FedRep	FedTrans	<i>Ours</i> : FedMT (P & L)	
5	8.56(0.33)	13.20(0.14)	16.89(0.74)	21.31(1.27)	<b>21.68</b> (0.67)	20.56(0.42)
10	12.29(0.32)	18.02(0.25)	21.90(1.27)	24.53(1.40)	<b>26.44</b> (0.34)	23.89(0.13)
15	14.34(0.15)	23.44(0.08)	23.39(0.67)	26.21(0.95)	<b>28.25</b> (0.34)	25.74(0.59)
20	16.23(0.21)	27.70(0.09)	24.70(0.55)	27.49(0.85)	<b>29.75</b> (0.66)	27.43(0.35)
25	17.73(0.20)	30.71(0.59)	26.53(0.29)	28.16(1.30)	30.63(0.06)	28.53(0.52)

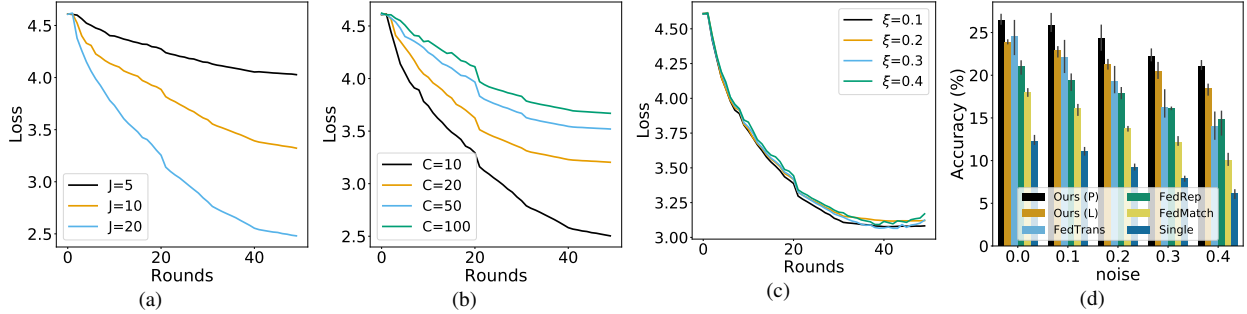


Figure 2: Ablation studies on CIFAR100. (a) Effects of the number of classes  $J$  on convergence. (b) Effects of the number of clients on convergence. (c) Effects of noise level  $\xi$  on convergence. (d) Study of performance accuracy with different noise levels on the server. All the convergence results are shown on the first 50 rounds using FedMT (L) for better visualization.

supervision is limited  $n < 25$ . We achieve similar but much more stable performance compared with FedMatch when  $n = 25$ . FedMatch adaptively augments the training data with labels in the desired label space using heuristically derived confident pseudo labels. Future work could combine FedMT with similar approaches used in FedMatch to evaluate heuristic results in a theoretically provable framework.

**Analysis on convergence** To validate our developed theoretical results in Theorem 3.4, we investigate the convergence rate of loss (2) of FedMT with label projection. In Fig. 2(a), we explore loss as a function of the number of classes  $J \in \{5, 10, 20\}$  with  $C = 10$  under noise-free setting, and the convergence is consistent with Corollary 3.5, smaller  $J$  leads to lower convergence. The loss curves in Fig. 2(b) show FedMT convergence was achieved faster when training with more clients for a fixed total number of samples. This result is consistent with the theoretical result of Theorem 3.4. As shown in Fig. 2(c), under the default setting, the convergence rates are similar at different noise levels. The results demonstrate our method is reasonably stable to noise, which is in line with Corollary 3.6.

**Effect of varying noise levels** Our method has the flexibility to adapt to the case where the server data is noisy. We use the accuracy of  $K$ -class prediction in the held out test set to compare our method with other approaches in CIFAR100, the results are reported in Fig. 2(d). Given the mislabeling rate in many real applications (e.g., healthcare) could be as high as 40% (Lettieri et al., 2005), we compare FedMT with other learning approaches, by varying the noise level  $\xi$  on the server from  $\{0, 0.1, 0.2, 0.3, 0.4\}$  and set  $n = 10$  on the server.<sup>4</sup> From the results, our proposed FedMT method significantly outperforms all alternative methods both even when the noise level  $\xi$  is up to 0.4. Second, when increasing noise levels, FedMT shows more stable performance compared to baselines. Our method also shows stable performance if we have more than 1 client has observations from desired label space and the results is given in Appendix D.5.

### 4.3 Tremor Severity Prediction of Parkinson’s Disease

**Dataset** Our method is not limited to sub- and super-classes as in CIFAR100, to illustrate the effectiveness of our method under the general overlapping class case, we evaluate FedMT for the prediction of tremor severity for patients with Parkinson’s disease (PD). Tremor is a typical movement disorder occurring on the limbs of patients with PD (Qin et al., 2020). Surface electromyography (sEMG) is widely used for movement disorder assessment by noninvasively recording electrical signals on the skin. The patterns of sEMG signals can be used to turn PD diagnosis into different subtypes based on the diagnostic values. We use the synthetic sEMG dataset in Qin et al. (2020). In our experiment,

<sup>4</sup>We assume the labels are sampled from known, systemic, and instance-independent noisy transition matrix  $T$ , whose diagonal values are  $1 - \xi$ . Our method can be extended to estimate  $T$  using anchor point-based methods (Scott, 2015; Liu and Tao, 2015) but discussing the estimation method is not in the scope of this work.



Table 2: Comparison of the accuracy for 5-class classification using our methods and alternative methods on the sEMG dataset with various  $n$  and  $C = 50$  under noise-free setting. We report mean (sd) from three trial runs. The best method is highlighted in boldface.

$n$	Single	FedMatch	FedRep	FedTrans	<i>Ours</i> : FedMT (P & L)	
1	27.30(0.88)	28.20(0.67)	39.34(1.12)	42.31(2.12)	<b>66.89</b> (0.91)	63.67(0.28)
2	30.83(1.30)	31.90(1.45)	40.49(1.16)	46.45(0.63)	<b>67.00</b> (0.38)	64.22(0.28)
3	34.66(1.09)	32.90(1.74)	41.29(1.16)	51.25(2.57)	<b>67.34</b> (0.57)	64.33(0.48)
4	39.11(1.48)	33.53(2.12)	43.24(0.68)	51.81(1.99)	<b>67.67</b> (0.64)	64.44(0.35)
5	42.57(0.78)	37.20(2.09)	44.24(0.74)	51.83(2.14)	<b>67.22</b> (0.30)	64.44(0.55)

we consider  $K = 5$  on the server and  $J = 3$  on the client, according to MDS-UPDRS19. Goetz et al. (2008)<sup>5</sup> In this dataset, the classes in two label spaces has overlap. The form of  $\mathbf{Q}$  is given in Appendix C.2.

**Setup** We randomly sample 9000 observations from the sEMG dataset as client training data. We hold out 1000 observations for testing. We then split the training set to  $C = 50$  clients completely at random, but ensuring that samples are balanced within each class in both label spaces. Each client, therefore, has roughly 60 observations from one of the three classes. In addition to the training set on clients, we also have  $n$  observations per class on the server. Similar to the benchmark experiment, we vary  $n$  on the server. Following Qin et al. (2019), we use 12 summary statistics of sEMG as our features: mean absolute value (MAV), mean square value (MSV), root mean square (RMS), variance (VAR), standard deviation (STD), waveform length (WL), Willison amplitude (WAMP), log detector (LOG), slope sign change (SSC), zero crossing (ZC), mean spectral frequency (MSF) and median frequency (MF). The mathematical definition of these features is given in Chowdhury et al. (2013). We then use a single hidden layer multiple layer perceptron (MLP) with 128 hidden units and ReLU activation function as our backbone. We use SGD optimizer with learning rate as  $10^{-3}$ , and set batch size as 16. Local update frequency is 1 epoch. We train the model for 100 communication rounds. More training details are available in Appendix C.2. We use the same performance measure and the same alternative approaches as those described in Section 4.1 for comparison.

**Results** Overall, our quantitative results in Tab. 2 show that FedMT with probability projection performs better than probability projection on the sEMG dataset and consistently outperforms alternative learning approaches. FedMT improves mean accuracy by a non-negligible margin, demonstrating a synergistic collaborative effect with clients’ data from the other label space. The superiority of FedMT in this demanding medical data setting further demonstrates the efficacy and robustness of our algorithm. To test of the performance of FedMT at different degree of overlapping, we also conduct experiments when  $K = 10$  with various noisy levels, the results is given in Appendix E. Our method also outperforms other methods in this case.

## 5 Conclusion

In this work, we propose a new FL framework, FedMT, to address an important yet under-explored mixed-type label setting. Theoretically, we provide the convergence guarantee of FedMT with the extension of NTK. Through extensive experiments on a benchmark and a medical dataset, we demonstrate FedMT can outperform alternative methods. We also emphasize that since FedMT makes minor modifications to local predictions or labels, it has much more flexibility to integrate with other FL strategies beyond FedAvg. The performance of our proposed method can be further improved by combining our provable method with other heuristic-based weakly supervised learning approaches. As a plug-and-play method, FedMT can be applied to non-IID setting by combining with advanced FL schemes, including Li et al. (2020b, 2021); Karimireddy et al. (2020).

## References

- Act, A. (1996). Health insurance portability and accountability act of 1996. *Public law*, 104:191.
- Alemohammad, S., Wang, Z., Balestrieri, R., and Baraniuk, R. (2020). The recurrent neural tangent kernel. *arXiv preprint arXiv:2006.10246*.
- Arora, S., Du, S. S., Hu, W., Li, Z., Salakhutdinov, R. R., and Wang, R. (2019). On exact computation with an infinitely wide neural net. *Advances in Neural Information Processing Systems*, 32.

<sup>5</sup>The labeling strategies are detailed in Appendix C.2

- Bdair, T., Navab, N., and Albarqouni, S. (2021). Fedperl: Semi-supervised peer learning for skin lesion classification. In *International Conference on Medical Image Computing and Computer-Assisted Intervention*, pages 336–346. Springer.
- Chen, J., Niu, L., Liu, L., and Zhang, L. (2021a). Weak-shot fine-grained classification via similarity transfer. *Advances in Neural Information Processing Systems*, 34:7306–7318.
- Chen, X., Wang, S., Fu, B., Long, M., and Wang, J. (2019). Catastrophic forgetting meets negative transfer: Batch spectral shrinkage for safe transfer learning. *Advances in Neural Information Processing Systems*, 32.
- Chen, Y., Liu, Z., Xu, H., Darrell, T., and Wang, X. (2021b). Meta-baseline: Exploring simple meta-learning for few-shot learning. In *Proceedings of the IEEE/CVF International Conference on Computer Vision*, pages 9062–9071.
- Chowdhury, R. H., Reaz, M. B., Ali, M. A. B. M., Bakar, A. A., Chellappan, K., and Chang, T. G. (2013). Surface electromyography signal processing and classification techniques. *Sensors*, 13(9):12431–12466.
- Collins, L., Hassani, H., Mokhtari, A., and Shakkottai, S. (2021). Exploiting shared representations for personalized federated learning. In *International Conference on Machine Learning*, pages 2089–2099. PMLR.
- Du, S. S., Hou, K., Salakhutdinov, R. R., Póczos, B., Wang, R., and Xu, K. (2019). Graph neural tangent kernel: Fusing graph neural networks with graph kernels. *Advances in neural information processing systems*, 32.
- Goetz, C. G., Tilley, B. C., Shaftman, S. R., Stebbins, G. T., Fahn, S., Martinez-Martin, P., Poewe, W., Sampaio, C., Stern, M. B., Dodel, R., et al. (2008). Movement disorder society-sponsored revision of the unified parkinson’s disease rating scale (MDS-UPDRS): scale presentation and clinimetric testing results. *Movement disorders: official journal of the Movement Disorder Society*, 23(15):2129–2170.
- He, K., Zhang, X., Ren, S., and Sun, J. (2016). Deep residual learning for image recognition. In *Proceedings of the IEEE conference on computer vision and pattern recognition*, pages 770–778.
- Hu, A., Sun, Z., and Li, Q. (2022). Weakly supervised fine-grained recognition based on combined learning for small data and coarse label. In *Proceedings of the 2022 International Conference on Multimedia Retrieval*, pages 194–201.
- Huang, B., Li, X., Song, Z., and Yang, X. (2021). FL-NTK: A neural tangent kernel-based framework for federated learning analysis. In *International Conference on Machine Learning*, pages 4423–4434. PMLR.
- Jacot, A., Gabriel, F., and Hongler, C. (2018). Neural tangent kernel: Convergence and generalization in neural networks. *Advances in neural information processing systems*, 31.
- Jeong, W., Yoon, J., Yang, E., and Hwang, S. J. (2021). Federated semi-supervised learning with inter-client consistency & disjoint learning. In *International Conference on Learning Representations*.
- Jiang, Y., Konečný, J., Rush, K., and Kannan, S. (2019). Improving federated learning personalization via model agnostic meta learning. *arXiv preprint arXiv:1909.12488*.
- Kairouz, P., McMahan, H. B., Avent, B., Bellet, A., Bennis, M., Bhagoji, A. N., Bonawitz, K., Charles, Z., Cormode, G., Cummings, R., et al. (2021). Advances and open problems in federated learning. *Foundations and Trends® in Machine Learning*, 14(1–2):1–210.
- Karimireddy, S. P., Kale, S., Mohri, M., Reddi, S., Stich, S., and Suresh, A. T. (2020). Scaffold: Stochastic controlled averaging for federated learning. In *International Conference on Machine Learning*, pages 5132–5143. PMLR.
- Khaled, A., Mishchenko, K., and Richtárik, P. (2020). Tighter theory for local sgd on identical and heterogeneous data. In *International Conference on Artificial Intelligence and Statistics*, pages 4519–4529. PMLR.
- Krizhevsky, A., Hinton, G., et al. (2009). Learning multiple layers of features from tiny images. Technical report, University of Toronto.
- Lee, J., Xiao, L., Schoenholz, S., Bahri, Y., Novak, R., Sohl-Dickstein, J., and Pennington, J. (2019). Wide neural networks of any depth evolve as linear models under gradient descent. *Advances in neural information processing systems*, 32.
- Legislature, C. S. (2018). California consumer privacy act (ccpa). <https://oag.ca.gov/privacy/ccpa>.

- Lettieri, C. J., Veerappan, G. R., Parker, J. M., Franks, T. J., Hayden, D., Travis, W. D., and Shorr, A. F. (2005). Discordance between general and pulmonary pathologists in the diagnosis of interstitial lung disease. *Respiratory medicine*, 99(11):1425–1430.
- Li, T., Sahu, A. K., Zaheer, M., Sanjabi, M., Talwalkar, A., and Smith, V. (2020a). Federated optimization in heterogeneous networks. *Proceedings of Machine Learning and Systems*, 2:429–450.
- Li, T., Sahu, A. K., Zaheer, M., Sanjabi, M., Talwalkar, A., and Smith, V. (2020b). Federated optimization in heterogeneous networks. *Proceedings of Machine Learning and Systems*, 2:429–450.
- Li, X., Huang, K., Yang, W., Wang, S., and Zhang, Z. (2019). On the convergence of fedavg on non-iid data. *arXiv preprint arXiv:1907.02189*.
- Li, X., Jiang, M., Zhang, X., Kamp, M., and Dou, Q. (2021). FedBN: Federated learning on non-iid features via local batch normalization. In *International Conference on Learning Representations*.
- Liu, T. and Tao, D. (2015). Classification with noisy labels by importance reweighting. *IEEE Transactions on pattern analysis and machine intelligence*, 38(3):447–461.
- Lu, N., Wang, Z., Li, X., Niu, G., Dou, Q., and Sugiyama, M. (2021). Unsupervised federated learning is possible. In *International Conference on Learning Representations*.
- Lu, N., Wang, Z., Li, X., Niu, G., Dou, Q., and Sugiyama, M. (2022). Unsupervised federated learning is possible.
- McKeown, R. E., Holbrook, J. R., Danielson, M. L., Cuffe, S. P., Wolraich, M. L., and Visser, S. N. (2015). The impact of case definition on attention-deficit/hyperactivity disorder prevalence estimates in community-based samples of school-aged children. *Journal of the American Academy of Child & Adolescent Psychiatry*, 54(1):53–61.
- McMahan, B., Moore, E., Ramage, D., Hampson, S., and y Arcas, B. A. (2017). Communication-efficient learning of deep networks from decentralized data. In *Artificial intelligence and statistics*, pages 1273–1282. PMLR.
- Patrini, G., Rozza, A., Krishna Menon, A., Nock, R., and Qu, L. (2017). Making deep neural networks robust to label noise: A loss correction approach. In *Proceedings of the IEEE conference on computer vision and pattern recognition*, pages 1944–1952.
- Qin, Z., Chen, J., Jiang, Z., Yu, X., Hu, C., Ma, Y., Miao, S., and Zhou, R. (2020). Learning fine-grained estimation of physiological states from coarse-grained labels by distribution restoration. *Scientific Reports*, 10(1):1–10.
- Qin, Z., Jiang, Z., Chen, J., Hu, C., and Ma, Y. (2019). sEMG-based tremor severity evaluation for Parkinson’s disease using a light-weight CNN. *IEEE Signal Processing Letters*, 26(4):637–641.
- Reddi, S., Charles, Z., Zaheer, M., Garrett, Z., Rush, K., Konečný, J., Kumar, S., and McMahan, H. B. (2020). Adaptive federated optimization. *arXiv preprint arXiv:2003.00295*.
- Rothchild, D., Panda, A., Ullah, E., Ivkin, N., Stoica, I., Braverman, V., Gonzalez, J., and Arora, R. (2020). Fetchsgd: Communication-efficient federated learning with sketching. In *International Conference on Machine Learning*, pages 8253–8265. PMLR.
- Ruder, S. (2016). An overview of gradient descent optimization algorithms. *arXiv preprint arXiv:1609.04747*.
- Scott, C. (2015). A rate of convergence for mixture proportion estimation, with application to learning from noisy labels. In *Artificial Intelligence and Statistics*, pages 838–846. PMLR.
- Touvron, H., Sablayrolles, A., Douze, M., Cord, M., and Jégou, H. (2021). Graft: Learning fine-grained image representations with coarse labels. In *Proceedings of the IEEE/CVF International Conference on Computer Vision*, pages 874–884.
- Van Rooyen, B. and Williamson, R. C. (2017). A theory of learning with corrupted labels. *J. Mach. Learn. Res.*, 18(1):8501–8550.
- Voigt, P. et al. (2018). The EU general data protection regulation (GDPR). *Intersoft consulting*.
- Yang, Q., Liu, Y., Chen, T., and Tong, Y. (2019). Federated machine learning: Concept and applications. *ACM Transactions on Intelligent Systems and Technology (TIST)*, 10(2):1–19.
- Yu, F., Rawat, A. S., Menon, A., and Kumar, S. (2020). Federated learning with only positive labels. In *International Conference on Machine Learning*, pages 10946–10956. PMLR.

## A Notation Table

Table 3: Important notations used in the paper.

Notations	Description
$d$	input dimension
$n$	number of per desired label space class samples on the server
$t$	local updating iterations
$C$	number of clients in the FL, we index client by $c \in [C]$
$J$	number of classes in the other label space
$K$	number of classes in the desired label space
$\mathbf{T}$	linear transformation of noisy labels on the server
$\mathbf{Q}$	linear transformation between two label spaces
$R$	aggregation communication rounds
$N_c$	size of samples on the $c$ -th client
$S_c$	the set of indices of observations on $c$ -th client
$\mathcal{X}$	input space $\mathcal{X} \subset \mathbb{R}^d$
$\tilde{\mathcal{Y}}$	the other label space $\tilde{\mathcal{Y}} = \{\tilde{Y}^1, \tilde{Y}^2, \dots, \tilde{Y}^J\}$
$\mathcal{Y}$	desired label space $\mathcal{Y} = \{Y^1, Y^2, \dots, Y^K\}$
$\mathcal{D}^c$	dataset $\mathcal{D}_c = \{(\mathbf{x}_i^c, y_i^c) : i \in S_c\}$ on $c$ -th client
$\mathcal{D}^s$	dataset on server $\mathcal{D}^s = \{(\mathbf{x}_i^s, y_i^s) : i \in [nK]\}$ where $y_i^s \in \mathcal{Y}_{\text{fine}}$
$\mathbf{x}$	inputs variable $\mathbf{x} \in \mathcal{X}$
$\mathbf{f}(\cdot)$	a classification model that assigns a score to each of the $K$ classes for a given input $\mathbf{x}$
$\ell(\cdot, \cdot)$	loss function for the classification task
$\hat{R}_c(\cdot)$	empirical risk on $c$ -th client
$\hat{R}_s(\cdot)$	empirical risk on the server
$\eta_{\text{local}}$	local GD step size
$\eta_{\text{agg}}$	aggregation step size
$\xi$	the noise level in $\mathbf{T}$

## B Technical Details of the Neural Tangent Kernel Analysis

In this section, we present the technical details of the Neural Tangent Kernel Analysis on the convergence of the algorithm of the label projection approach. We first present the NTK analysis of a simple regression model with weighted loss. We then show how the conclusion be extended to our classification case under FL.

### B.1 NTK with Weighted MSE Loss for Regression

Let us first consider an over-parameterized one-hidden layer neural network (NN) for regression. Let  $f : \mathcal{X} \rightarrow \mathbb{R}$  be the output of the NN with the form

$$f(\mathbf{u}, \mathbf{x}) = \frac{1}{\sqrt{M}} \sum_{m=1}^M a_m \phi(\mathbf{u}_m^\top \mathbf{x})$$

where  $\phi(z) = \max\{z, 0\}$  is the ReLU activation function and  $\mathbf{u} = [\mathbf{u}_1, \mathbf{u}_2, \dots, \mathbf{u}_M] \in \mathbb{R}^{d \times M}$ . Let  $\mathcal{D} = \{(\mathbf{x}_i, y_i) : i \in [n]\}$  be a set of training examples. We consider the learning  $f$  under the following weighted MSE loss

$$\mathcal{L}(\mathbf{u}) = \frac{1}{2} \sum_{i=1}^n w_i (f(\mathbf{u}, \mathbf{x}_i) - y_i)^2.$$

Let  $\eta$  be the learning rate of gradient descent algorithm, the evolution of the parameters  $\mathbf{u}$  and the  $f$  via continuous time gradient descent satisfies

$$\begin{aligned}\frac{df(\mathbf{u}(t), \mathbf{x}_i)}{dt} &= \frac{\partial f(\mathbf{u}(t), \mathbf{x}_i)}{\partial \mathbf{u}^\top} \frac{d\mathbf{u}(t)}{dt}, \\ \frac{d\mathbf{u}(t)}{dt} &= -\eta \sum_{i=1}^n \frac{\partial f(\mathbf{u}(t), \mathbf{x}_i)}{\partial \mathbf{u}} \frac{\partial \mathcal{L}}{\partial f(\mathbf{u}(t), \mathbf{x}_i)}\end{aligned}\quad (8)$$

based on the chain rule.

Let  $f(\mathbf{u}, \mathcal{D}) = (f(\mathbf{u}, \mathbf{x}_1), f(\mathbf{u}, \mathbf{x}_2), \dots, f(\mathbf{u}, \mathbf{x}_n))^T$ . Given the weighted MSE loss, we have

$$\frac{\partial \mathcal{L}}{\partial f(\mathbf{u}, \mathcal{D})} = (w_1(f(\mathbf{u}, \mathbf{x}_1) - y_1), w_2(f(\mathbf{u}, \mathbf{x}_2) - y_2), \dots, w_n(f(\mathbf{u}, \mathbf{x}_n) - y_n))^\top$$

and

$$\frac{\partial f(\mathbf{u}, \mathcal{D})}{\partial \mathbf{u}} = \left( \frac{\partial f(\mathbf{u}, \mathbf{x}_1)}{\partial \mathbf{u}^\top}, \frac{\partial f(\mathbf{u}, \mathbf{x}_2)}{\partial \mathbf{u}^\top}, \dots, \frac{\partial f(\mathbf{u}, \mathbf{x}_n)}{\partial \mathbf{u}^\top} \right)^\top.$$

Hence, we get

$$\frac{df(\mathbf{u}, \mathbf{x}_i)}{dt} = -\eta \sum_{j=1}^n w_j \frac{\partial f(\mathbf{u}, \mathbf{x}_i)}{\partial \mathbf{u}^\top} \frac{\partial f(\mathbf{u}, \mathbf{x}_j)}{\partial \mathbf{u}} \{f(\mathbf{u}, \mathbf{x}_j) - y_j\}.$$

Then the full evolution dynamic of learning  $f$  is

$$\frac{df(\mathbf{u}(t), \mathcal{D})}{dt} = -\eta \mathbf{\Lambda}(t) (f(\mathbf{u}(t), \mathcal{D}) - \mathbf{y})$$

where  $\mathbf{y} = (y_1, y_2, \dots, y_n)^\top$ , the Gram matrix  $\mathbf{\Lambda}(t) \in \mathbb{R}^{n \times n}$  is

$$\mathbf{\Lambda}(t) = \nabla_{\mathbf{u}} f(\mathbf{u}(t), \mathcal{D}) W \nabla_{\mathbf{u}}^\top f(\mathbf{u}(t), \mathcal{D}),$$

and  $W = \text{diag}(w_1, w_2, \dots, w_n)$ .

## B.2 NTK under Weighted MSE Loss for Classification

With the preparation in Section B.1, we now show the NTK kernel under the weighted MSE loss for classification. We first consider the centralized version and then extend the conclusions to the federated learning case.

**Centralized Classification** To make the presentation easier, we first introduce some notations. Let  $\mathcal{D} = \{(\mathbf{x}_i, \mathbf{y}_i) : i \in [n]\}$  be a set of training examples where  $\mathbf{y}_i$  is the one-hot representation of the label. Let  $\mathbf{f} : \mathcal{X} \mapsto \mathbb{R}^K$  be a  $K$ -class classifier and  $\mathbf{g}(\mathbf{u}, \mathbf{x}) = \sigma(\mathbf{f}(\mathbf{u}, \mathbf{x}))$ . In this section, we show the evolution dynamic of learning  $\mathbf{g}$  under the following weighted MSE loss

$$\mathcal{L}(\mathbf{u}) = \sum_{i=1}^n \mathcal{L}_i(\mathbf{u}) = \frac{1}{2} \sum_{i=1}^n \sum_{j=1}^J \sum_{k=1}^K Q_{jk}^{-1} \{y_{ik} - g_k(\mathbf{u}, \mathbf{x}_i)\}^2$$

where  $\mathbf{Q}^{-1} \in \mathbb{R}^{J \times K}$  is a known matrix and  $Q_{jk}^{-1}$  is the  $(j, k)$ -th element of  $\mathbf{Q}^{-1}$ .

Following (8), the evolution of the parameters  $\mathbf{u}$  and the output  $\mathbf{g}$  via continuous time gradient descent satisfies

$$\begin{aligned}\frac{dg_k(\mathbf{u}(t), \mathbf{x}_i)}{dt} &= \frac{\partial g_k(\mathbf{u}(t), \mathbf{x}_i)}{\partial \mathbf{u}^\top} \frac{d\mathbf{u}(t)}{dt} \\ \frac{d\mathbf{u}(t)}{dt} &= -\eta \sum_{l=1}^n \sum_{\kappa=1}^K \frac{\partial g_\kappa(\mathbf{u}(t), \mathbf{x}_l)}{\partial \mathbf{u}} \frac{\partial \mathcal{L}_l(\mathbf{u}(t))}{\partial g_\kappa}\end{aligned}\quad (9)$$

Under the weighted MSE loss, we have

$$\frac{\partial \mathcal{L}_l(\mathbf{u}(t))}{\partial g_\kappa} = \sum_{j=1}^J Q_{jk}^{-1} \{g_\kappa(\mathbf{u}, \mathbf{x}_l) - y_{l\kappa}\}.$$

Plug in the gradient to (9), we have

$$\frac{dg_k(\mathbf{u}(t), \mathbf{x}_i)}{dt} = -\eta \sum_{l=1}^n \sum_{\kappa=1}^K \sum_{j=1}^J \frac{\partial g_k(\mathbf{u}(t), \mathbf{x}_i)}{\partial \mathbf{u}^\top} \frac{\partial g_\kappa(\mathbf{u}(t), \mathbf{x}_l)}{\partial \mathbf{u}} Q_{j\kappa}^{-1} \{g_\kappa(\mathbf{u}, \mathbf{x}_l) - y_{l\kappa}\}$$

Let  $\mathbf{g}(\mathbf{u}, \mathcal{D}) = \sigma(\mathbf{f}(\mathbf{u}, \mathcal{D})) = (g_1(\mathbf{u}, \mathbf{x}_1), \dots, g_1(\mathbf{u}, \mathbf{x}_n), \dots, g_K(\mathbf{u}, \mathbf{x}_1), \dots, g_K(\mathbf{u}, \mathbf{x}_n))^\top$ , and

$$\mathbf{y} = (y_{11}, \dots, y_{n1}, \dots, y_{1K}, \dots, y_{nK})^\top.$$

Then in the matrix form, the full evolution dynamic of learning  $\mathbf{g}$  becomes

$$\frac{d\mathbf{g}(\mathbf{u}(t), \mathcal{D})}{dt} = -\eta \mathbf{H}(t)(\mathbf{g}(\mathbf{u}(t), \mathcal{D}) - \mathbf{y})$$

where the Gram matrix  $\mathbf{H}(t) \in \mathbb{R}^{Kn \times Kn}$  is a block matrix with  $K$  row partitions and  $K$  column partitions. The  $(p_1, p_2)$ -th element of the block matrix in the  $l$ -th row and  $m$ -th column has the following form

$$\mathbf{H}_{p_1, p_2}^{l, m}(t) = \sum_{j=1}^J Q_{jm}^{-1} \frac{\partial g_l(\mathbf{u}(t), \mathbf{x}_{p_1})}{\partial \mathbf{u}^\top} \frac{\partial g_m(\mathbf{u}(t), \mathbf{x}_{p_2})}{\partial \mathbf{u}}. \quad (10)$$

**Federated Classification** We can now extend the study of the full evolution dynamic of learning  $\mathbf{g}$  under centralized version to federated classification. For federated learning case, we have the following datasets: the set of training examples  $\mathcal{D}^c = \{(\mathbf{x}_i^c, \mathbf{y}_i^c) : i \in S_c\}$  on  $c$ -th client where  $\mathbf{y}_i$  is the one-hot representation of the label in dimension  $K$  and the training data on the server  $\mathcal{D}^s = \{(\mathbf{x}_i^s, \mathbf{y}_i^s) : i \in [nK]\}$  where  $\mathbf{y}_i^s$  is the one-hot representation of the label. Let  $\mathbf{f} : \mathcal{X} \mapsto \mathbb{R}^K$  be a  $K$ -class classifier. We consider the learning of  $\mathbf{f}$  under the mean squared error loss

$$\mathcal{L}_c(\mathbf{u}) = \frac{1}{2} \sum_{i=1}^n \sum_{j=1}^J \sum_{k=1}^K Q_{jk}^{-1} \{y_{ik}^c - g_k(\mathbf{u}, \mathbf{x}_i^c)\}^2, \quad \mathcal{L}_s(\mathbf{u}) = \frac{1}{2} \sum_{i=1}^{nK} \sum_{k'=1}^K \sum_{k=1}^K T_{k'k}^{-1} \{y_{ik}^s - g_k(\mathbf{u}, \mathbf{x}_i^s)\}^2.$$

The overall loss is

$$\mathcal{L}(\mathbf{u}) = \mathcal{L}_s(\mathbf{u}) + \sum_{c=1}^C \mathcal{L}_c(\mathbf{u}). \quad (11)$$

Same as the centralized case, let us consider the evolution of  $\mathbf{g}$  via continuous time gradient descent.

$$\begin{aligned} \frac{dg_k(\mathbf{u}(t), \mathbf{x}_i)}{dt} &= \frac{\partial g_k(\mathbf{u}(t), \mathbf{x}_i)}{\partial \mathbf{u}^\top} \frac{d\mathbf{u}(t)}{dt} \\ \frac{d\mathbf{u}(t)}{dt} &= -\eta \sum_l \sum_{\kappa=1}^K \frac{\partial g_\kappa(\mathbf{u}(t), \mathbf{x}_l)}{\partial \mathbf{u}} \frac{\partial \mathcal{L}_l(\mathbf{u}(t))}{\partial g_\kappa} \end{aligned}$$

The difference of our federated version from the centralized version is  $\partial \mathcal{L} / \partial g_\kappa$ . Under (11), we have

$$\frac{\partial \mathcal{L}_l(\mathbf{u}(t))}{\partial g_\kappa} = \begin{cases} \sum_{j=1}^J Q_{j\kappa}^{-1} \{g_\kappa(\mathbf{u}, \mathbf{x}_l) - y_{l\kappa}\} & \text{if } \mathbf{x}_l \text{ on } c\text{-th client,} \\ \sum_{k'=1}^K T_{k'\kappa}^{-1} \{g_\kappa(\mathbf{u}, \mathbf{x}_l) - y_{l\kappa}\} & \text{if } \mathbf{x}_l \text{ on the server.} \end{cases}$$

Hence we have

$$\begin{aligned} \frac{dg_k(\mathbf{u}(t), \mathbf{x}_i)}{dt} &= -\eta \sum_{i'=1}^{nK} \sum_{\kappa=1}^K \frac{\partial g_k(\mathbf{u}(t), \mathbf{x}_i)}{\partial \mathbf{u}^\top} \frac{\partial g_\kappa(\mathbf{u}(t), \mathbf{x}_{i'})}{\partial \mathbf{u}} \sum_{k'=1}^K T_{k'\kappa}^{-1} \{g_\kappa(\mathbf{u}, \mathbf{x}_{i'}) - y_{i'\kappa}^s\} \\ &\quad - \eta \sum_{c=1}^C \sum_{i' \in S_c} \sum_{\kappa=1}^K \frac{\partial g_k(\mathbf{u}(t), \mathbf{x}_i)}{\partial \mathbf{u}^\top} \frac{\partial g_\kappa(\mathbf{u}(t), \mathbf{x}_{i'}^c)}{\partial \mathbf{u}} \sum_{j=1}^J Q_{j\kappa}^{-1} \{g_\kappa(\mathbf{u}, \mathbf{x}_{i'}^c) - y_{i'\kappa}^c\}. \end{aligned}$$

To write the evolution of  $\mathbf{g}$  in matrix form, let us first introduce some notations. Let

$$\mathbf{g}_k(\mathbf{u}, \mathcal{D}) = (g_k(\mathbf{u}, \mathbf{x}_1^1), \dots, g_k(\mathbf{u}, \mathbf{x}_{N_1}^1), \dots, g_k(\mathbf{u}, \mathbf{x}_1^C), \dots, g_k(\mathbf{u}, \mathbf{x}_{N_C}^C), g_k(\mathbf{u}, \mathbf{x}_1^s), \dots, g_k(\mathbf{u}, \mathbf{x}_{nK}^s))^\top$$

and  $\mathbf{g}(\mathbf{u}, \mathcal{D}) = (g_1^\top(\mathbf{u}, \mathcal{D}), \dots, g_K^\top(\mathbf{u}, \mathcal{D}))^\top$ . Note the vector  $\mathbf{g}(\mathbf{u}, \mathcal{D})$  is first grouped by machines and then classes. Similarly, we also denote  $\mathbf{y}^k = (y_{1k}^1, \dots, y_{N_1,k}^1, \dots, y_{1k}^C, \dots, y_{N_C,k}^C, y_{1k}^s, \dots, y_{n_K,k}^s)$  and  $\mathbf{y} = (\mathbf{y}^1, \mathbf{y}^2, \dots, \mathbf{y}^K)$ . Then in the matrix form, the full evolution dynamic of learning  $\mathbf{g}$  becomes

$$\frac{d\mathbf{g}(\mathbf{u}(t), \mathcal{D})}{dt} = -\eta \mathbf{G}(t)(\mathbf{g}(\mathbf{u}(t), \mathcal{D}) - \mathbf{y})$$

where the Gram matrix  $\mathbf{G}(t) \in \mathbb{R}^{K(nK+N) \times K(nK+N)}$  is a block matrix with  $K$  row partitions and  $K$  column partitions. The block matrix in the  $l$ -th row and  $m$ -th column has the following form

$$\mathbf{G}^{l,m}(t) = \begin{pmatrix} \mathcal{G}_{1,1}^{l,m}(t) & \mathcal{G}_{1,2}^{l,m}(t) & \dots & \mathcal{G}_{1,C}^{l,m}(t) & \mathcal{G}_{1,s}^{l,m}(t) \\ \mathcal{G}_{2,1}^{l,m}(t) & \mathcal{G}_{2,2}^{l,m}(t) & \dots & \mathcal{G}_{2,C}^{l,m}(t) & \mathcal{G}_{2,s}^{l,m}(t) \\ \vdots & \vdots & \ddots & \vdots & \vdots \\ \mathcal{G}_{C,1}^{l,m}(t) & \mathcal{G}_{C,2}^{l,m}(t) & \dots & \mathcal{G}_{C,C}^{l,m}(t) & \mathcal{G}_{C,s}^{l,m}(t) \\ \mathcal{G}_{s,1}^{l,m}(t) & \mathcal{G}_{s,2}^{l,m}(t) & \dots & \mathcal{G}_{s,C}^{l,m}(t) & \mathcal{G}_{s,s}^{l,m}(t) \end{pmatrix}$$

for  $l \in [K]$  and  $m \in [K]$ . The block matrix  $\mathbf{G}^{l,m}(r)$  is also consisted of block matrices. The block matrix  $\mathcal{G}_{c_1,c_2}^{l,m}(t) \in \mathbb{R}^{N_{c_1} \times N_{c_2}}$ ,  $\mathcal{G}_{s,c}^{l,m}(t) \in \mathbb{R}^{n_K \times N_c}$ , and  $\mathcal{G}_{s,s}^{l,m}(t) \in \mathbb{R}^{n_K \times n_K}$  for  $c_1 \in [C]$ ,  $c_2 \in [C]$ , and  $c \in [C]$ .

We now specify the elements in  $\mathcal{G}_{c_1,c_2}^{l,m}(t)$ ,  $\mathcal{G}_{s,c}^{l,m}(t)$ , and  $\mathcal{G}_{s,s}^{l,m}(t)$  respectively. The derivation is the same as (10). We have

- The  $(p_1, p_2)$ -th element of  $\mathcal{G}_{c_1,c_2}^{l,m}(t)$  has the following form

$$\sum_{j=1}^J Q_{jm}^{-1} \frac{\partial g_l(\mathbf{u}, \mathbf{x}_{p_1}^{c_1})}{\partial \mathbf{u}^\top} \frac{\partial g_m(\mathbf{u}, \mathbf{x}_{p_2}^{c_2})}{\partial \mathbf{u}}.$$

- The  $(p_1, p_2)$ -th element of  $\mathcal{G}_{s,c}^{l,m}(t)$  has the following form

$$\sum_{j=1}^J Q_{jm}^{-1} \frac{\partial g_l(\mathbf{u}, \mathbf{x}_{p_1}^s)}{\partial \mathbf{u}^\top} \frac{\partial g_m(\mathbf{u}, \mathbf{x}_{p_2}^c)}{\partial \mathbf{u}}.$$

- The  $(p_1, p_2)$ -th element of  $\mathcal{G}_{s,s}^{l,m}(t)$  has the following form

$$\sum_{k=1}^K T_{km}^{-1} \frac{\partial g_l(\mathbf{u}, \mathbf{x}_{p_1}^s)}{\partial \mathbf{u}^\top} \frac{\partial g_m(\mathbf{u}, \mathbf{x}_{p_2}^s)}{\partial \mathbf{u}}.$$

### B.3 Proof of Corollaries

In this section, we provide the proof for Corollary 3.5 and Corollary 3.6.

**Proof for Corollary 3.6** The key for the proof is to find the form of  $\mathbf{T}^{-1}$  when  $\mathbf{T} = (1 - K\xi/(K-1))\mathbb{I}_K + \xi/(K-1)\mathbb{I}_K\mathbb{I}_K^\top$ . To find  $\mathbf{T}^{-1}$ , we make use of the Woodbury matrix identity

$$(\mathbf{A} + \mathbf{UCV})^{-1} = \mathbf{A}^{-1} - \mathbf{A}^{-1}\mathbf{U}(\mathbf{C}^{-1} + \mathbf{VA}^{-1}\mathbf{U})^{-1}\mathbf{VA}^{-1}$$

where  $\mathbf{A}$ ,  $\mathbf{U}$ ,  $\mathbf{C}$ , and  $\mathbf{V}$  are matrices of proper sizes.

In our case,  $\mathbf{A} = \{1 - K\xi/(K-1)\}\mathbb{I}_K$ ,  $\mathbf{U} = \mathbb{I}_K$ ,  $\mathbf{C} = \xi/(K-1)$ , and  $\mathbf{V} = \mathbb{I}_K^\top$ . By applying Woodbury matrix identity, we get

$$\mathbf{T}^{-1} = (K-1)/(K-1-K\xi)\mathbb{I}_K - \xi/(K-1-K\xi)\mathbb{I}_K\mathbb{I}_K^\top.$$

Hence

$$\sum_{k=1}^K T_{kk'} = (\mathbf{T}^{-1}\mathbb{I}_K)_k = ((K-1)/(K-1-K\xi)\mathbb{I}_K - \xi/(K-1-K\xi)\mathbb{I}_K\mathbb{I}_K^\top)_k = (\mathbb{I}_K)_k = 1$$

which completes the proof.

**Proof for Corollary 3.5** Let  $k_1, k_2, \dots, k_J$  be  $J$  non-negative integers such that  $K = \sum_{j=1}^J k_j$ . If the linear transformation from desired label space to the other label space is  $\mathbf{Q} = \text{diag}(\mathbf{1}_{k_1}, \mathbf{1}_{k_2}, \dots, \mathbf{1}_{k_J}) \in [0, 1]^{K \times J}$  (i.e., the classes in the desired label space are sub-classes of the class in the other label space), then the smaller the value of  $J$ , the lower the convergence rate.

We will use the following conclusion (Li et al., 2021) in the proof. For a block positive definite matrix  $\mathbf{A} = (\mathbf{A}_{ij})_{n \times n}$ , we must have

$$\lambda_{\min}(\mathbf{A}) \leq \min_i \lambda_{\min}(\mathbf{A}_{ii}).$$

By recursively using this conclusion on  $\mathbf{G}(t)$  given in (7). We have

$$\lambda = \lambda_{\min}(\mathbf{G}(0)) \leq \min_{k,c,s} \{\lambda_{\min}(\mathcal{G}_{c,c}^{k,k}(0)), \lambda_{\min}(\mathcal{G}_{s,s}^{k,k}(0))\} \leq \min_{k,c} \lambda_{\min}(\mathcal{G}_{c,c}^{k,k}(0)).$$

Let  $\lambda_0^c = \lambda_{\min}(\nabla_{\mathbf{u}} g_k(\mathbf{u}(0), \mathcal{D}^c) \nabla_{\mathbf{u}} g_k^\top(\mathbf{u}(0), \mathcal{D}^c))$  for  $c \in [C]$ . Under the special case where the two label spaces have hierarchical structures, we have  $\mathbf{Q}^{-1} = \text{diag}(k_1^{-1} \mathbb{1}_{k_1}^\top, k_2^{-1} \mathbb{1}_{k_2}^\top, \dots, k_J^{-1} \mathbb{1}_{k_J}^\top)$

Since  $\mathcal{G}_{c,c}^{k,k}(0) = \left\{ \sum_j \mathbf{Q}_{jk}^{-1} \right\} \nabla_{\mathbf{u}} g_k(\mathbf{u}(0), \mathcal{D}^c) \nabla_{\mathbf{u}} g_k^\top(\mathbf{u}(0), \mathcal{D}^c)$ , it is easy to see that

$$\lambda_{\min}(\mathcal{G}_{c,c}^{k,k}(0)) \leq \left\{ \min_j k_j^{-1} \right\} \lambda_0^c.$$

where  $\lambda_0^c$  is a constant, the smallest eigen value of  $\nabla_{\mathbf{u}} g_k(\mathbf{u}(0), \mathcal{D}^c) \nabla_{\mathbf{u}} g_k^\top(\mathbf{u}(0), \mathcal{D}^c)$  (i.e., the original kernel of FL-NTK Huang et al. (2021)), which does not depend on  $J$ .

Hence

$$\lambda \leq \min_c \left\{ \min_j k_j^{-1} \right\} \lambda_0^c.$$

Since  $\sum_j k_j = K$ , and in our setting we have  $k_1 \approx k_2 \approx \dots \approx k_J$ , the smaller the value of  $J$ , the smaller the value of  $\lambda$  and hence the algorithm converges slower.

## C Experimental Details

We present our model architectures and training details of the benchmark and synthetic sEMG medical dataset in this section.

### C.1 Model Architecture and Implementation Details on Benchmark

The details of the experiments on the benchmark CIFAR100 dataset are presented in this section.

**Model architecture** For our benchmark experiments on CIFAR100, we use ResNet18 as our backbone. The network details are listed in Tab. 4.

**Data split and label Generation** Here, we describe how to prepare the CIFAR100 training dataset into sub-class but noisy data on the server and super-class datasets on the clients. We first select  $n$  samples from each of the  $K = 100$  sub-classes as the datasets on the server. To generate noisy labeled data at noise level  $\xi \in [0, 1]$ , we assume that the noise matrix is known, symmetric, instance independent, and reconstructable, represented as the matrix  $\mathbf{T}_\xi = \{1 - K/(K-1)\xi\} \mathbb{I}_K + \xi/(K-1) \mathbb{1}_K \mathbb{1}_K^\top$ . Then the observed labels are sampled from this given matrix by random flipping, i.e., the label in one class is flipped to the label in another class with probability  $\xi/(K-1)$ . The higher the value of  $\xi$ , the larger the proportion of noise labels. Then for the rest of the observations in the CIFAR100 training set, we randomly split then into  $C$  pieces each with  $N_c$  observations and each client is assigned  $N_c$  samples. Hence in this case  $\mathbf{Q}$  is a  $200 \times 100$  matrix, its  $(j, i)$ -th element is 1 if the  $i$ -th class is in  $j$ -th superclass and 0 otherwise.

**Training details** We implement all the methods by PyTorch and conducted all the experiments on an NVIDIA Tesla V100 GPU. For our FedMT, we use SGD optimizer Ruder (2016) with a learning rate of  $10^{-2}$ , momentum 0.9, and weight decay  $5 \times 10^{-4}$ . Each model updates one epoch then aggregates with the others. The total communication iterations is set to be 100. The learning rate is divided by 5 at 20, 30, and 40 iterations. We set the batch size to 16 and the number of training examples on  $c$ -th client to  $N_c = 4000$  if not specified otherwise. In Tab. 1, we consider various values for the per number of observations  $n$  on the server under the noise-free setting. We also consider various values



Table 4: Model architecture of the benchmark experiment on CIFAR100. For convolutional layer (Conv2D), we list parameters with sequence of input and output dimension, kernel size, stride and padding. For max pooling layer (MaxPool2D), we list kernel and stride. For fully connected layer (FC), we list input and output dimension. For BatchNormalization layer (BN), we list the channel dimension.

Layer	Details
1	Conv2D(3, 64, 7, 2, 3), BN(64), ReLU
2	Conv2D(64, 64, 3, 1, 1), BN(64), ReLU
3	Conv2D(64, 64, 3, 1, 1), BN(64)
4	Conv2D(64, 64, 3, 1, 1), BN(64), ReLU
5	Conv2D(64, 64, 3, 1, 1), BN(64)
6	Conv2D(64, 128, 3, 2, 1), BN(128), ReLU
7	Conv2D(128, 128, 3, 1, 1), BN(64)
8	Conv2D(64, 128, 1, 2, 0), BN(128)
9	Conv2D(128, 128, 3, 1, 1), BN(128), ReLU
10	Conv2D(128, 128, 3, 1, 1), BN(64)
11	Conv2D(128, 256, 3, 2, 1), BN(128), ReLU
12	Conv2D(256, 256, 3, 1, 1), BN(64)
13	Conv2D(128, 256, 1, 2, 0), BN(128)
14	Conv2D(256, 256, 3, 1, 1), BN(128), ReLU
15	Conv2D(256, 256, 3, 1, 1), BN(64)
16	Conv2D(256, 512, 3, 2, 1), BN(512), ReLU
17	Conv2D(512, 512, 3, 1, 1), BN(512)
18	Conv2D(256, 512, 1, 2, 0), BN(512)
19	Conv2D(512, 512, 3, 1, 1), BN(512), ReLU
20	Conv2D(512, 512, 3, 1, 1), BN(512)
21	AvgPool2D
22	FC(512, 100)

for the noisy level  $\xi$  when  $n = 10$ . For additional results in the Appendix D, we specify the hyper-parameters only when they are different.

We describe details of the baseline methods and corresponding hyper-parameters as follows.

- **Single** For this baseline method, we only use the limited data on the server to train a  $K$ -class classifiers. Under the noisy label scenarios, we also apply the label projection and the probability projection on the server and the learning objectives is

$$\widehat{R}(\mathbf{f}) = -\frac{1}{nK} \sum_{i=1}^{nK} \sum_{k=1}^K \mathbb{1}(y_i^s = Y^k) \log \left\{ \sum_{k'=1}^K T_{kk'} \sigma(f_{k'}(\mathbf{x}_i^s)) \right\},$$

for probability projection and

$$\widehat{R}(\mathbf{f}) = -\frac{1}{nK} \sum_{i=1}^{nK} \sum_{k=1}^K \left\{ \sum_{k'=1}^K T_{kk'}^{-1} \mathbb{1}(y_i^s = Y^{k'}) \right\} \log \sigma(f_k(\mathbf{x}_i^s)),$$

for label projection. We use the same optimizer as our FedMT.

- **FedMatch** We use the semi-supervised FedMatch proposed by (Lu et al., 2021). We treat client samples as unlabeled data, perform pseudo-labeling on the unlabeled sets under the supervision of labeled data on the server. The pseudo-labels are updated heuristically during the training. The data augmentation strategy is also used. For fair comparison, we do not use the pretrained backbone during training. We set learning rate to 0.01, batch size to 16, and the rest of the hyperparameters are the same as the default setting in the implementation.

- **FedRep** (Collins et al., 2021) For this baseline method, all clients train a super-class classifier and the server trains a sub-class classifier that differs in the last layer with different output dimension. The learning objective is

$$\hat{R}(\mathbf{f}) = \frac{1}{C} \sum_{c=1}^{C+1} \left\{ \hat{R}_c(\mathbf{f}; \mathcal{D}^c) + \hat{R}_s(\mathbf{f}; \mathcal{D}^s) \right\},$$

where

$$\hat{R}_c(\mathbf{f}; \mathcal{D}^c) = -\frac{1}{N_c} \sum_{i \in S_c} \sum_{j=1}^J \mathbb{1}(y_i = \tilde{Y}^j) \log \sigma(f_j(\mathbf{x}_i))$$

and  $\hat{R}_s(\mathbf{f}; \mathcal{D}^s)$  is the same as the objective function in the Single baseline approach. All classifiers on the server and on the clients use the same ResNet18 backbone, but they have different last layers. For the classifiers on clients, their last layer is FC(512,20); for the classifier on the server, its last layer is FC(512,100). The last layers of classifiers on clients are also not shared during the training. The rest of the parameters of all classifiers are aggregated using FedAvg during training. We use the same optimizer as our FedMT.<sup>6</sup>

- **FedTrans** For this baseline method, we first pretrain a model using the client data to train a  $J$ -class classifiers using FedAvg with probability projection or label projection. This pretrained net is then fine-tuned on the server. During the fine-tuning, we add a new linear layer with  $K$  classes with random initialization and backbone is initialized with the pretrained model. We use the same optimizer as our FedMT during the pretrain step and the model is fine-tuned on the server for 100 epochs with SGD optimizer and learning rate 0.01.

## C.2 Model Architecture and Implementation Details on Medical Dataset

**Model architecture** We use a simple MLP as the model for the medical data, whose architecture is listed in Table 5.

Table 5: Model architecture of the experiment on medical dataset sEMG. For fully connected layer (FC), we list input and output dimension. For BatchNormalization layer (BN), we list the channel dimension.

Layer	Details
1	FC(12,128), BN(128), ReLU
2	FC(128, 10)

**Data Preprocessing** The raw sEMG data is collected from Qin et al. (2020), with the dimensionality of 2048, *i.e.*, 2048 time points per sample,  $\mathbf{x} = [x_1, \dots, x_{2048}]$ . Following Qin et al. (2019), instead of using the raw time series, we use the extracted features as described in Section 4. The features twelve hand-crafted features, including mean absolute value (MAV), mean square value (MSV), root mean square (RMS), variance (VAR), standard deviation (STD), waveform length (WL), Willison amplitude (WAMP), log detector (LOG), slope sign change (SSC), zero crossing (ZC), mean spectral frequency (MSF) and median frequency (MF). Denote  $P_j$  is the sEMG power spectrum at frequency bin  $j$ , and  $f_j$  is the frequency of the sEMG power spectrum at frequency bin  $j$ . Mathematically, these features are defined in Tab. 6

We randomly sample 9000 samples as training data annotated with label from the other label space, and 1000 samples as the held testing data. We set the number of clients  $C = 50$ , namely each client has 180 samples. The data are labeling based on the severity value from 0 to 5. We equally partition the values into 3 parts with the same intervals (*i.e.*,  $[0, 5/3)$ ,  $[5/3, 10/3)$ , and  $[10/3, 5]$ ) corresponding to  $J = 3$  labeled classes on the clients. Such class partition strategy can simulate the overlapped case between two label spaces, where samples in the same  $Y^k$  class can belong to different  $\tilde{Y}^j$  classes. From the remaining sEMG samples, we randomly sample  $n$  observations per 5 class to represent the data on server. Under the noisy label scenarios, the noisy labels are generated using the same protocol as described in Section C.1.

<sup>6</sup>Note that the data labeling settings, models, and evaluation methods implemented in our work is adjusted to make fair comparison with other methods and different from those in Collins et al. (2021).

Table 6: Mathematical representation of widely used sEMG feature extraction methods. The constant  $\zeta$  is an user specified threshold and we set  $\zeta = 1$ .

Feature Extraction	Mathematical Equation
mean absolute value (MAV)	$\frac{1}{N} \sum_{n=1}^N  x_n $
mean square value (MSV)	$\frac{1}{N} \sum_{n=1}^N x_n^2$
root mean square (RMS)	$\sqrt{\frac{1}{N} \sum_{n=1}^N x_n^2}$
variance (VAR)	$\frac{1}{N-1} \sum_{n=1}^N x_n^2$
standard deviation (STD)	$\sqrt{\frac{1}{N-1} \sum_{n=1}^N x_n^2}$
waveform length (WL)	$\sum_{n=1}^{N-1}  x_{n+1} - x_n $
Willison amplitude (WAMP)	$\sum_{n=1}^{N-1} f( x_{n+1} - x_n ); f(x) = \begin{cases} 1 & \text{if } x \geq \zeta \\ 0 & \text{otherwise} \end{cases}$
log detector (LOG)	$\exp\left(\frac{1}{N} \sum_{n=1}^N \log  x_n \right)$
slope sign change (SSC)	$\sum_{n=2}^{N-1} f[(x_n - x_{n-1}) \times (x_n - x_{n+1})]; f(x) = \begin{cases} 1 & \text{if } x \geq \zeta \\ 0 & \text{otherwise} \end{cases}$
zero crossing (ZC)	$\sum_{n=1}^{N-1} [\text{sgn}(x_n \times x_{n+1}) \cap  x_n - x_{n+1}  \geq \zeta]; \text{sgn}(x) = \begin{cases} 1 & \text{if } x \geq \zeta \\ 0 & \text{otherwise} \end{cases}$
mean spectral frequency (MSF)	$\frac{\sum_{j=1}^M f_j P_j}{\sum_{j=1}^M P_j}$
median frequency (MF)	$\frac{1}{2} \sum_{j=1}^M P_j \quad \mathcal{X} \subset \mathbb{R}^d$

**Training details** We implement all the methods by PyTorch and conducted all the experiments on an NVIDIA Tesla V100 GPU. All the methods are trained for 100 round and each round, model update once before aggregation. We use SGD optimizer Ruder (2016) with a learning rate of  $10^{-2}$ , momentum 0.9, and weight decay  $5 \times 10^{-4}$ . The learning rate is divided by 5 at 20, 30, and 40 epochs. We set the batch size to 16. We also consider various values for the noisy level  $\xi$  from 0 to 0.4. All the experiments are repeated with independent random seeds.

## D More Experimental Results on CIFAR100

In this section, we present more experiment results on the benchmark CIFAR100 dataset. In Section D.1, we show the convergence of the loss function as a function of batch sizes and the local rounds. In Section D.2, we show the experiment results of our FedMT when different weighting schemes are used for server and clients. In Section D.3, we show the experiment results as the number of per client observation increases. In Section D.4, we study the performance of our proposed method under label heterogeneous across clients. In Section D.5, we show the performance of our method when limited data from desired label space are further split into more pieces.

### D.1 Effects of Local Rounds and Batch Size

To demonstrate the robustness of the proposed FedMT and validate our developed theoretical results in Theorem 3.4, we investigate the effects of different local rounds  $t$  and the batch size  $B$  on training losses (2) of FedMT with label projection in Section 4.1. For all experiments, the learning rate is set to be 0.0001 and no learning rate scheduler is used during the training. In Fig. 3(a), we explore loss as a function of the batch size  $B \in \{16, 64, 128\}$  with  $C = 10$  and without noise on super-class labels. The larger the batch size, the faster the loss function converges. In Fig. 3(b), we explore loss as a function of the local rounds  $t \in \{1, 4, 8\}$  with  $C = 10$  and without noise on super-class labels. The larger the local rounds, the faster the convergence, which is consistent with the theoretical result of Theorem 3.4. It is worth noting that all the training curves of different variants of the parameters reach convergence.

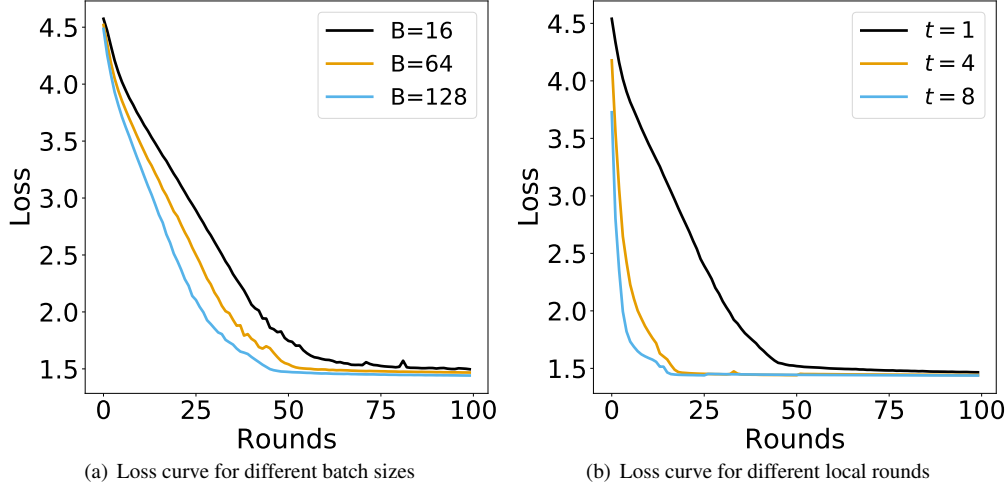


Figure 3: Effects of (a) the batch size  $B$  and (b) the local rounds  $t$  on the rate of convergence on the loss function.

## D.2 Benchmark Experiments with Weighted FedMT

In our main results, the loss on the each client and the loss on the server are equally weighted with weight  $1/(C+1)$ . To see the performance of our FedMT, we also investigate the case when these losses are weighted unequally and report the classification accuracy of the corresponding trained model on the held out test set in Tab. 7. For these experiment results, we consider different number of  $n \in \{5, 10, 20, 40, 80\}$  with  $\xi = 0.2$ . The sample size on  $c$ -th client  $N_c = 4000$ . For the unequal weight case, the weight on the server is 0.5 regardless of the size of  $n$  and the weight on each client is  $0.5/C$ . As shown in the table, the test classification accuracy increases with  $n$  for both equally weighted and unequally weighted cases. The performance of the unequally weighted case is not as good as the equally weighted case.

Table 7: Comparison of the accuracy for 100-class classification using different FL aggregation strategies on CIFAR100 benchmark dataset at different number of per  $K$  class training examples  $n$  when noise level  $\xi = 0.2$ . We report mean (sd) from three trial runs.

Weights	Methods	5	10	20	40	80
Equal	Our (P)	19.70(0.30)	24.26(0.85)	27.48(0.48)	30.56(0.61)	34.85(0.12)
	Our (L)	18.10(0.41)	21.26(0.32)	24.37(0.26)	28.28(0.18)	32.15(0.86)
Unequal	Our (P)	19.27(0.20)	21.49(0.50)	23.83(0.12)	26.66(0.11)	29.25(0.25)
	Our (L)	13.16(0.62)	14.40(0.21)	16.09(0.22)	19.15(0.25)	21.61(0.33)

## D.3 Benchmark Experiments with More Clients

In Tab. 1, we check the performance of our proposed method for varying amount of data on the server. In this section, we present the performance of our proposed method under varying amount of data on the client when  $n = 10$  and  $\xi = 0.2$  on the server. We also set the per client number of observations to be  $N_c = 800$ . We change the number of clients  $C \in \{10, 20, 30, 40, 50\}$ . The larger the number of clients  $C$ , more data we have. During the aggregation, we set the weights of the server to be 0.5 and the rest of the client to be  $0.5/C$ . In comparison, if the equal weight  $1/(C+1)$  is used, the super-class data on the server plays a less importance role as  $C$  increases. We therefore use the unequally weighted strategy to avoid. The classification result of the aggregated model on the held out test set is given in Table 8. As shown in the table, the classification accuracy increases as the number of clients increases.

Table 8: Our FedMT classification accuracy on benchmark CIFAR100 with different number of clients.

Methods	10	20	30	40	50
Our (P)	13.61(0.16)	15.17(0.29)	15.28(0.11)	15.92(0.44)	16.32(0.27)

## D.4 Benchmark Experiments under Non-IID Data Split

The heterogeneity of the training data across clients is a major challenge in FL Kairouz et al. (2021). We therefore study the performance of our method under two different FL settings: IID and non-IID. The overall label distribution across clients is the same in the IID setting, whereas clients have different label distributions in the non-IID setting. For the IID setting, we split the sub-class label training data evenly to all clients completely at random. For the non-IID setting, we split the dataset to clients as follows:

- the classes are divided into the majority and minority classes, where the fraction of each minority class is less than 0.08 while the fraction of each majority class is in the range [0.15, 0.25];
- the training data for every client are sampled from 2 majority classes and rest from minority classes;

We compare our method with personalized FL method FedRep both under noise-free and label noise on the server. We

Table 9: Comparison of the accuracy for 100-class classification using our methods and FedRep on the CIFAR100 benchmark dataset under IID and non-IID data split. We report mean (sd) from three trial runs.

$\xi$	0.0	0.1	0.2	0.3	0.4
IID					
Our (P)	26.44(0.34)	25.88(0.67)	24.26(0.85)	22.25(0.41)	21.04(0.33)
FedRep	21.00(0.45)	19.34(0.57)	17.89(0.37)	16.16(0.08)	14.80(0.89)
Non-IID					
Our (P)	21.40(0.21)	20.37(0.28)	20.14(0.26)	18.72(0.45)	17.44(0.39)
FedRep	20.71(0.58)	18.45(0.69)	17.11(0.35)	14.73(0.25)	13.74(0.13)

make the following comparisons: 1) the performance of our method under IID case and non-IID case. 2) the performance of our method under non-IID case and FedRep under non-IID case. 3) the performance of our method under non-IID case and other baselines under IID case. Since our aggregation is based on FedAvg, it can be seen from the table that there is a 4-5% performance drop of our proposed method when data on the clients are non-IID. However, it is worth noticing that our proposed method under non-IID case works better than other baselines under IID case. Moreover, our proposed method still outperforms FedRep when both approaches are applied on non-IID data split. Therefore, the above experiment results show the robustness of our proposed method compared with other approaches.

## D.5 Different Number of “Servers”

In our problem setting, we assume without loss of generality that there is one ‘specialized center’ with a small amount of data from desired label space and we call this center as the server. Such a setting is motivated by the real clinical application in Section 1 that “the centers with the most complex labeling criteria...has much less labeled samples due to labeling difficulty or cost”. It is technically trivial to generalize our problem to the case with several entities with data from desired label space by simplify modifying Equation 11 as

$$R_{\text{overall}}(\mathbf{f}) = \frac{1}{C + S} \left\{ \sum_{s=1}^S \hat{R}_s(\mathbf{f}; \tilde{\mathcal{D}}^s) + \sum_{c=1}^C \hat{R}_c(\mathbf{f}; \tilde{\mathcal{D}}^c) \right\}$$

where  $\tilde{\mathcal{D}}^s$  is the noisy labeled data on  $s$ -th server and  $S$  is the total number of such servers. To show the effectiveness of our proposed method under this setting, we run the following experiments on CIFAR100. We have  $C = 10$  clients with super-class clean data with each client having  $N_c = 4000$  samples. We also have  $n = 20$  noisy sub-class data. We consider the following 3 ways to store these  $20 \times 100$  images: 1) we have one “server” with all noisy sub-class images. 2) we have 2 “server”s with each containing  $n = 10$  noisy sub-class images. 3) we have 4 “server”s with each containing  $n = 5$  noisy sub-class images. We change the level of noise  $\xi \in \{0.1, 0.2, 0.3, 0.4, 0.5\}$  and show the results for both FedMT(P) and FedMT(L). It can be seen from the table that an increase in the number of “server”s does not hurt the performance of FedMT(P) and there is a slight performance drop for FedMT(L).

## D.6 Sensitivity analysis of projection matrix

In this section, we show the experiment on testing the robustness of our proposed method to the perturbation of the transition matrix  $T$ . Following Lu et al. (2022), we let

$$\tilde{T} = T \odot \{(2\epsilon - 1)P + 1\}$$

Table 10: Comparison of the accuracy for 100-class classification using FedMT(P) on the CIFAR100 benchmark dataset with different split strategy of the sub-class label at different noise level  $\xi$ . We report mean (sd) from three trial runs.

Split	0.1	0.2	0.3	0.4
Our (P)				
1x20	28.26(0.88)	27.48(0.48)	26.36(0.84)	24.36(1.47)
2x10	29.11(0.21)	27.88(0.62)	26.38(1.09)	24.16(0.27)
4x5	28.13(0.36)	27.26(0.37)	24.64(0.63)	23.37(0.36)
Our (L)				
1x20	27.53(0.71)	24.37(0.26)	23.78(0.50)	22.45(0.73)
2x10	25.64(0.52)	24.08(0.29)	22.29(0.71)	20.67(0.43)
4x5	23.88(0.30)	22.58(0.50)	21.52(0.18)	20.51(0.20)

where each element in  $\mathbf{P}$  are IID random variables from  $[0, 1]$  and  $\odot$  is the elementwise product between two matrices. We then standard  $\mathbf{T}$  so that its column sum is 1. We have run the experiments with  $\epsilon \in \{0.1, 0.5, 0.9\}$  for different noise levels and the experiment results is given in Tab. 11. The last row of the table is the experiment result with the true  $\mathbf{T}$ . It can be seen from the figure that our proposed method FedMT is robust to a perturbation of the projection matrix  $\mathbf{T}$ .

Table 11: Sensitivity analysis when the projection matrix  $\mathbf{T}$  is perturbed under different noise levels  $\xi$  on CIFAR100. We let  $C = 10$ ,  $N_c = 4000$  and  $n = 10$  in the experiment. The value of  $\epsilon$  denotes the degree of perturbation, the larger the value of  $\xi$ , the higher the degree of perturbation. The last row is the test accuracy with the true  $\mathbf{T}$ .

$\epsilon$	$\xi = 0.0$	$\xi = 0.1$	$\xi = 0.2$	$\xi = 0.3$
0.1	25.44	23.95	22.27	21.72
0.5	24.89	24.37	22.57	21.68
0.9	24.73	24.13	22.52	20.81
True $\mathbf{T}$	25.99	25.15	22.95	21.71

## E More Experimental Results on Tremor Severity Prediction

For the experiment on tremor severity prediction in Section 4.3, we let  $K = 5$  and the  $\mathbf{Q}$  matrix between two label spaces is

$$\mathbf{Q} = \begin{bmatrix} 3/5 & 2/5 & 0 & 0 & 0 \\ 0 & 1/5 & 3/5 & 1/5 & 0 \\ 0 & 0 & 0 & 2/5 & 3/5 \end{bmatrix}.$$

There are 2 out of 5 classes in the desired space overlaps with one of the class in the other space, each with degree of overlapping  $1/5 = 20\%$ . To investigate the performance of various approaches under different degrees of overlapping, we create the labels on the servers as below. We equally partition the values into 10 parts with the same intervals (i.e.,  $[0.5k, 0.5k + 0.5)$  for  $k \in \{0, 2, \dots, 9\}$ ) and keep  $J = 3$  and the corresponding labels the same as before. In this case, the  $\mathbf{Q}$  matrix between two label spaces becomes

$$\mathbf{Q} = \begin{bmatrix} 3/10 & 3/10 & 3/10 & 1/10 & 0 & 0 & 0 & 0 & 0 & 0 \\ 0 & 0 & 0 & 1/5 & 3/10 & 3/10 & 1/5 & 0 & 0 & 0 \\ 0 & 0 & 0 & 0 & 0 & 0 & 1/10 & 3/10 & 3/10 & 3/10 \end{bmatrix}$$

Under this case, there are 2 out of 10 classes in the desired space overlaps with one of the class in the other space, each with degree of overlapping is  $1/10 = 10\%$ . As a comparison and additional experiment results, we compare the performance of all methods for different values of  $K$  under the case when there are noisy labels on the server. We let  $n = 3$  and the rest of the settings the same as before. The experiment results are given in Tab. 12. It is shown in the table that our method can beat the rest of the methods regardless of the noise level.

Table 12: Comparison of the accuracy using our methods and alternative methods on the sEMG dataset with  $n = 3$  and  $K = 5$  that has smaller degree of class overlapping and  $K = 10$  that has larger degree of class overlapping. We conduct the experiment when  $C = 50$  at different noise level  $\xi$ . We report mean (sd) from three trial runs. The best method is highlighted in boldface.

$\xi$	Single	FedMatch	FedRep	FedTrans	<i>Ours</i> : FedMT (P&L)	
larger degree of overlapping						
0.0	22.35(2.31)	13.04(1.79)	29.23(2.31)	28.75(1.21)	28.97(0.32)	32.59(1.81)
0.1	21.12(2.34)	13.14(0.76)	21.12(2.34)	27.73(1.72)	28.86(0.73)	30.60(1.16)
0.2	18.75(1.68)	12.51(2.19)	18.75(1.68)	25.95(0.99)	27.63(1.05)	30.26(1.69)
0.3	17.49(1.50)	10.54(1.07)	17.49(1.50)	21.56(2.04)	27.00(0.42)	28.16(1.53)
0.4	14.25(1.17)	11.64(1.17)	14.25(1.17)	18.00(2.15)	27.03(1.48)	28.96(1.39)
smaller degree of overlapping						
0.0	34.39(2.86)	34.07(1.32)	41.12(1.34)	51.25(2.57)	67.34(0.56)	64.33(0.48)
0.1	31.04(2.69)	33.03(0.99)	39.64(1.62)	45.52(2.15)	61.80(0.24)	66.56(0.57)
0.2	30.77(1.89)	32.37(1.21)	37.66(1.80)	41.07(1.45)	61.34(0.30)	66.00(0.57)
0.3	27.41(3.02)	31.36(0.99)	34.37(3.38)	39.10(1.31)	61.26(0.31)	67.22(0.30)
0.4	24.66(2.59)	27.56(1.26)	27.09(2.03)	37.01(3.15)	66.44(0.41)	63.74(0.27)

## F Properties of Baselines for Comparison

For the empirical experiments in the paper, we compare the performance of our proposed method with several baseline approaches, namely Single, FedRep, FedMatch, and FedTrans. The details of these approaches and their corresponding objective functions are given in Appendix C. As a summary, we highlight their properties in Table 13 in terms of the type of labels they use on the server and clients, their learning strategy, whether they are simple extensions of FedAvg, and whether the theoretical guarantee on the convergence of the algorithm has been established. For the server label,

Table 13: The conceptual comparison of the baseline approaches with our proposed method in terms of the type of labeled information used on server and clients, the learning strategy, whether the approach is a simple extension of FedAvg, and whether there is a theoretical guarantee on the convergence of the algorithm.

	Server Label	Client Label	Strategy	Simple	Theory
Single	Desired	NA	supervised	Yes	Yes
FedMatch	Desired	Yes	semi-supervised	No	No
FedRep	Desired	Other	supervised	Yes	No
FedTrans	Desired	Other	supervised	Yes	No
Ours	Desired	Other	supervised	Yes	Yes

NA means the server label is not used and Desired means datasets are annotated with classes from the desired label space. For the client label, NA means the client label is not used, Other means datasets annotated with classes from the other label space are used, and Desired class prior means only the information of the prior distribution of the desired label space class labels is used. The second last column means whether the proposed method is a simple extension of FedAvg and the last column means whether the theoretical convergence of the method has been established under FL. For methods that are simple extensions of FedAvg, the communication cost is in general much cheaper than other more complicated approaches.